The p–n junction under nonuniform strains: general theory and application to photovoltaics

Laurent Guin, Michel Jabbour, Nicolas Triantafyllidis

Journal of the Mechanics and Physics of Solids 110 (2018) 54–79

Contents lists available at ScienceDirect

Journal of the Mechanics and Physics of Solids

journal homepage: www.elsevier.com/locate/jmps

The $p-n$ junction under nonuniform strains: general theory and application to photovoltaics

L. Guin[a,b], M.E. Jabbour[a,c], N. Triantafyllidis[a,c,d,*]

[a] LMS, École Polytechnique, CNRS, Université Paris-Saclay, Palaiseau 91128, France
[b] LPICM, École Polytechnique, CNRS, Université Paris-Saclay, Palaiseau 91128, France
[c] Département de Mécanique, École Polytechnique, Palaiseau 91128, France
[d] Aerospace Engineering Department & Mechanical Engineering Department(emeritus), The University of Michigan, Ann Arbor, MI 48109-2140, USA

ARTICLE INFO

Article history:
Received 4 May 2017
Revised 5 September 2017
Accepted 5 September 2017
Available online 6 September 2017

Keywords:
Coupled mechanical, electrical and electronic processes
Electrochemical potential
Deformable semiconductor materials

ABSTRACT

It is well known that mechanical strains influence the electronic properties of semiconductor devices. Modeling the fully coupled mechanical, electrical, and electronic responses of semiconductors is therefore essential for predicting the effects of mechanical loading on their overall electronic response. In the first part of this paper, we develop a general continuum model that couples the mechanical, electrical, and electronic responses of a finitely deformable semiconductor. The proposed model accounts for the dependence of the band edge energies, densities of states, and electronic mobilities on strain. The governing equations are derived from the basic principles of the thermomechanics of electromagnetic continua undergoing electronic transport. In particular, we find that there exists electronically induced strains that can exceed their electromagnetic (Maxwell) counterparts by an order of magnitude. In the second part, motivated by applications that involve the bending of a photovoltaic cell, we use asymptotic methods to compute the current–voltage characteristic of a $p-n$ junction under nonuniform strains. We find that, for a typical monocrystalline silicon solar cell, the changes in dark current are significant, i.e., of the order of 20% for strains of 0.2%.

1. Introduction

The discovery of semiconductors is one of the most significant scientific and technological breakthroughs of the second half of the twentieth century. Mechanical effects play an important role in the behavior of semiconductors, as first discovered by Bardeen and Shockley (1950). Strains were subsequently put to use in applications such as piezoresistors (Barlian et al., 2009), metal-oxide-semiconductor field-effect transistors (MOSFETs) which incorporate strained silicon technology to exploit the mobility enhancement induced by specific types of uniaxial stresses (Chu et al., 2009; Thompson et al., 2004; 2006), and quantum-well lasers, for which the changes induced in the band structure result in significant improvements of their performance (Adams, 2011; Coleman, 2000).

Different aspects of the coupling between the mechanical and electronic responses of semiconductors have been investigated by solid-state physicists and mechanicians. The emphasis in the first community is on scale bridging, i.e., predicting the influence of strain on the macroscopic properties, based on the electronic band structure. The second group, using

* Corresponding author at: LMS, École Polytechnique, 91128 Palaiseau, France.
E-mail address: nick@lms.polytechnique.fr (N. Triantafyllidis).

http://dx.doi.org/10.1016/j.jmps.2017.09.004
0022-5096/

methods of continuum mechanics and thermodynamics, has developed theoretical models of the coupled electro-mechanical problem. The goal of the present work is to derive, while using ideas from solid-state physics, a thermodynamically consistent and fully coupled continuum model of finitely deformable semiconductors, and, motivated by photovoltaics, to use this model to compute the current–voltage characteristic of a $p-n$ junction under strain gradients.

In the solid-state physics literature, starting with the work of Bardeen and Shockley (1950), theoretical studies have addressed the effect of strain on the band structure of a semiconductor. The band structure, associated with the atomic lattice, determines the characteristics of the distribution and motion of electrons and holes in the semiconductor (Kittel, 2004). Modifications of the atomic lattice geometry due to mechanical strains induce changes in the band energy levels, described by *deformation potentials*, and in the densities of states of the bands (Bardeen and Shockley, 1950; Bir et al., 1974; Fischetti and Laux, 1996; Herring and Vogt, 1956). These changes in the band structure affect, in turn, the mobilities of charge carriers, which are responsible for the semiconductor's *piezoresistive effect* (Kanda, 1991; Kleimann et al., 1998; Smith, 1954).

Aside from the dependence of electronic parameters on strain, it was found that the presence of a *nonuniform* strain field in a semiconductor changes the nature of the electronic transport. Indeed, standard models of electronic transport rely on the assumption of spatial homogeneity of the semiconductor, whereas the presence of nonuniform strains result in a *inhomogeneous* semiconductor. While Bardeen and Shockley (1950) noticed early on the possibility of "*gradual shifts in energy bands resulting from deformations of the crystal lattice*," it is Kroemer (1957) who introduced the notion of *quasi-electric field* to account for the effects of spatial gradients in material properties (band's energy level, density of states) on the electronic transport, giving as an example of an inhomogeneous semiconductor "*a semiconductor under nonuniform elastic strain*." Later, the drift–diffusion equations modeling the electron and hole transport were generalized to inhomogeneous semiconductors (Manku and Nathan, 1993; Marshak and Vliet, 1984; Marshak and van Vliet, 1978) by adding two new drift terms involving the gradient of the conduction and valence band edge energies and the gradient of densities of states. These generalizations were derived from fundamental computations based on the Boltzmann transport equation for free carriers in inhomogeneous semiconductors.

In addition to strain-induced changes in the electronic properties of the semiconductor itself, studies were carried out on the effect of uniform strains on the electronic response of a semiconductor device: *the piezojunction effect*. Both experimentally and with microscopic models, the piezojunction effect was studied for devices such as the $p-n$ junction (see e.g., Wortman et al., 1964; Wortman and Hauser, 1966; Kanda, 1967) and, more recently, the transistor in the thorough work of Creemer and French (2000) (see also Creemer et al., 2001; Creemer, 2002). It was found that strains of the order of 10^{-3} can change the current in the device by about ten percent. These works are concerned with devices at the scale of the micrometer for which classical models are valid. Recently, Freund and Johnson (2001) (see also Johnson et al., 1998; Johnson and Freund, 2001) addressed the influence of strain on electronic devices at the nanometer scale for which a quantum mechanical description becomes necessary. Their approach solves in two steps the mechanics and electronics problems. First the boundary-value problem (BVP) associated with the purely mechanical response is solved, the result of which is then used to write the Schrödinger equation for the wave-function of electrons with perturbations induced by the strain field. In our analysis of the $p-n$ junction in Section 3, we develop such a two-step approach in the framework of classical models of electronic transport, which has not been carried out before.

In all the above studies, mostly in the solid-state physics literature, the question considered concerns the influence a strain field has on the electronic transport properties of a semiconductor. However, the mechanical, electrostatic and electronic responses of semiconductors interact through mutual couplings. In the mechanics literature, semiconductors are modeled as continua, leading to boundary-value problems where the mechanical, electrostatic and electronic fields are coupled. This was done by de Lorenzi and Tiersten (1975), who developed a theory of the fully coupled problem where the unknown fields consist of the strain field, the electromagnetic field, and the free carriers distributions. The governing equations of the coupled problem are established by writing the general principles of mechanics, electromagnetism and electronics, and restrictions on the form of the constitutive relations are derived from thermodynamics. However, in this work, no explicit form is given for the constitutive relations, which makes it difficult to establish a connection with the governing equations used in semiconductor physics. This point is addressed in Section 2.3 of the present work.

More recently, Xiao and Bhattacharya (2008) derived a theory of the deformable semiconductor in the context of semiconducting ferroelectrics, their main focus being on the polarization dependence of strain and the associated phase changes. Whereas one can find common features between the general theory developed by these authors and ours, the couplings addressed are not the same. In particular, as a result of their neglect of strain effects on electronic properties, the chemical potential that appears in their model is, unlike ours, independent of strain.

Finally, in relation to the mathematical analysis of continuum models for electronic transport in rigid semiconductors, we refer the reader to the book of Markowich (1986) and the papers of Markowich and Ringhofer (1984) and Please (1982). Given that boundary-value problems of semiconductor devices are singularly perturbed at the interfaces (e.g., at $p-n$ interfaces), these authors developed asymptotic methods to address the existence and analytical computation of solutions to these problems.

In the present work, we first derive a fully coupled electrostatic–electronic–mechanical theory of deformable semiconductors wherein the thermodynamically consistent formulation of the interaction between electric field and polarizable matter is combined with the modeling of the transport of carrier charges. Specializing to crystalline semiconductors and using results of mechanics, electromagnetism and statistical physics, a functional form of the free energy—from which the constitutive relations derive—is proposed. This establishes a link with applications and provides a different insight into the

transport equations of the semiconductor physics literature. In the derivation of constitutive relations, a new mechanism is uncovered: the electronic state (electron and hole densities) contributes to the mechanical equilibrium through a new term in the total stress. The interest of writing the equations of the fully coupled problem, along with explicit constitutive relations, is that the orders of magnitude of the mechanical, electrostatic and electronic effects can be compared. We find that, for crystalline silicon, effect of the electronics and electrostatics on the mechanical equilibrium can be neglected. This explains why, in applications of interest, the mechanical problem can be solved independently, while there remains, as the coupling of importance, the effect of strain on the electronic transport. We hence justify the implicit assumption of the solid-state physics literature that the effect of strain on electronics can be studied on its own, noting that, in other settings to be determined, the electronic contribution to the stress could become significant.

Following the development of the general theory, we consider an application in which strain non-uniformity plays an essential role. Motivated by the strain effects on the performance of photovoltaic cells—for which uniform strain have been shown to play a role (Lange et al., 2016)—we compute the current–voltage response of a $p-n$ junction subjected to nonuniform strains which result from bending. Using asymptotic expansions of the generalized drift–diffusion equations, we compute, to leading order in strain, the changes in current–voltage characteristic. We show that the effect of nonuniform strain is equivalent to that of a uniform strain evaluated at a particular mid-point of the $p-n$ junction. With this result, we compute the change in dark current of a typical monocrystalline silicon solar cell and find variations up to twenty percent for strains of the order of 0.2%.

The remainder of this article is organized as follows: in Section 2, we derive a continuum theory of deformable semiconductors, that accounts for coupling between mechanics, electrostatics and charge-carrier transport. The balance laws are formulated in Section 2.1 and restrictions on the constitutive relations are obtained in Section 2.2. Section 2.3 specializes to crystalline semiconductors by providing explicit forms of the constitutive relations. We then compute in Section 3 the strain-induced change in the current–voltage characteristic of a $p-n$ junction under bending. The electronic transport problem is set in a one-dimensional framework in Section 3.1 and then solved using asymptotic methods in Section 3.2. The results are applied in Section 3.3 to determine the change in the dark current of a typical monocrystalline silicon solar cell deformed on a curved surface. Details of the 3D-to-1D reduction of the electronic parameters and the choice of the resulting 1D coefficients for silicon are given in Appendix A, while the asymptotic expansions are detailed in Appendix B.

2. Continuum formulation for deformable semiconductors

In this section, we derive the field equations that govern the mechanical, electromagnetic and electronic responses of a finitely deformable semiconductor. Denote by $\mathcal{B}_0$ and $\mathcal{B}_t$ the regions of space occupied by the semiconductor in the reference and current configurations, respectively. A material point with position $\mathbf{X}$ in the reference configuration is mapped at time t to the spatial point $\mathbf{x}=\chi(\mathbf{X},t)$.

The semiconductor consists of a continuum with electron-donor and electron-acceptor impurities, rigidly bound to it, with concentrations[1] $N_d(\mathbf{x},t)$ and $N_a(\mathbf{x},t)$, respectively. Since the impurities are bound to the continuum, the dependence on time of the functions $N_d(\mathbf{x},t)$ and $N_a(\mathbf{x},t)$ is solely due to convection. We assume that the donors and acceptors are ionized (an assumption that is valid in practice at room temperature for silicon, see Sze and Ng, 2006), so that the nuclei induce a volume charge density $q\rho C$ where q is the elementary charge, $\rho(\mathbf{x},t)$ the mass density and $C(\mathbf{x},t)$ is defined by

$$C := N_d - N_a. \tag{2.1}$$

Charge transport in the semiconductor occurs through free carriers, which consist of electrons (of charge $-q$) and holes (of charge q) moving freely in the conduction and valence bands, respectively. Note that the holes, located as they are in the valence band, represent an absence of electrons in that band. The two bands spread over the entire semiconductor and the concentrations of electrons in the conduction band and of holes in the valence band are denoted by $n(\mathbf{x},t)$ and $p(\mathbf{x},t)$, respectively. As a result, the charge density reads

$$q\rho(C+p-n). \tag{2.2}$$

In addition to the spatial motion of electrons and holes within their bands, it is possible for an electron to jump locally between the valence and conduction bands, an event represented by the recombination or generation of an electron–hole pair. Aside from the charges of impurities, the bound charges due to the polarizability of the material are accounted for by the specific polarization $\mathbf{P}(\mathbf{x},t)$ which represents dipole moment per unit mass.

Given that material velocities in deformable semiconductors are negligible with respect to the speed of light and restricting attention to electrical loading at sufficiently low frequency, the magnetic effects are expected to be negligible compared to the electric ones. We hence ignore all the magnetic fields (magnetic field, magnetic induction, magnetization).

In establishing the field governing equations, we write the balance laws in the current configuration on *material control volumes* $\mathcal{P}_t \subseteq \mathcal{B}_t$. To model the coupling between the mechanics and the electric field, we follow the approach of Kovetz (2000),[2] while the energetics associated with the transport of free carriers is written in the vein of the works of Gurtin and Vargas (1971) and Fried and Gurtin (1999); 2004) on the transport of chemical species. These works, and

[1] Throughout the paper, *concentration* denotes number of particles (atoms, ions, electrons or holes) per unit mass.

[2] For the equivalence between alternative formulations of the balance laws for electromagnetic continua see Steigmann (2009).

consequently the present one, follow the philosophy of the Coleman–Noll procedure (Coleman and Noll, 1963) to obtain information on the constitutive relations.

Note that for tensor calculus we follow the coordinate-free dyadic notation: for any vector fields $\mathbf{v}(\mathbf{x}, t)$ and $\mathbf{w}(\mathbf{x}, t)$ and rank-2 tensor fields $\mathbf{T}(\mathbf{x}, t)$ and $\mathbf{R}(\mathbf{x}, t)$, we have in a Cartesian basis:

$$\begin{cases} (\nabla\mathbf{v})_{ij} = v_{j,i}, & (\mathbf{v}\nabla)_{ij} = v_{i,j}, & (\nabla\cdot\mathbf{v}) = v_{i,i}, & (\nabla\cdot\mathbf{T})_i = T_{ji,j}, \\ (\mathbf{v}\mathbf{w})_{ij} = v_i w_j, & (\mathbf{T}\cdot\mathbf{v})_i = T_{ij}v_j, & \mathbf{T}\cdot\cdot\mathbf{R} = T_{ik}R_{ki}, & \mathbf{T} : \mathbf{R} = T_{ik}R_{ik}. \end{cases} \tag{2.3}$$

2.1. General principles

First, we write the general principles: the laws of electromagnetism and the usual balance laws of continuum mechanics and thermodynamics.

2.1.1. Maxwell equations

Let $\mathbf{d}(\mathbf{x}, t)$ be the electric displacement related by definition to the electric field $\mathbf{e}(\mathbf{x}, t)$ and specific polarization $\mathbf{P}(\mathbf{x}, t)$ by

$$\mathbf{d} = \epsilon_0\mathbf{e} + \rho\mathbf{P}, \tag{2.4}$$

where ϵ_0 is the vacuum permittivity. Where the fields are sufficiently smooth, local form of Gauss's law reads

$$\nabla\cdot\mathbf{d} = q\rho(C + p - n). \tag{2.5}$$

Further, under the hypothesis of negligible magnetic fields, Maxwell–Faraday's law has the form

$$\nabla \times \mathbf{e} = \mathbf{0}, \tag{2.6}$$

from which we infer the existence of an electric potential $\varphi(\mathbf{x}, t)$ defined up to a constant by

$$\mathbf{e} = -\nabla\varphi. \tag{2.7}$$

Finally, denoting by $\jmath(\mathbf{x}, t)$ the total current density—of conduction and convection—of free charges, Ampère's law, in view of the negligible magnetic fields, reduces to

$$\frac{\partial\mathbf{d}}{\partial t} = -\boldsymbol{\jmath}. \tag{2.8}$$

Note that Maxwell equations are valid not only in the semiconductor but in surrounding space as well.

2.1.2. Mass conservation

Assuming that electrons and holes have no mass, the integral form of mass conservation reads

$$\frac{\mathrm{d}}{\mathrm{d}t}\int_{\mathcal{P}_t} \rho \,\mathrm{d}v = 0, \tag{2.9}$$

which, by the Reynolds transport theorem, yields the local form

$$\dot\rho + \rho(\nabla\cdot\dot{\mathbf{x}}) = 0, \tag{2.10}$$

where the superposed dot denotes the material time derivative.

2.1.3. Balance of free carriers

Let $\jmath_n(\mathbf{x}, t)$ be the current density of free electrons (number of electrons per unit time and surface area) and denote by $R(\mathbf{x}, t)$ the source/sink term[3] that accounts for the creation and destruction of electrons in the conduction band due to the recombination–generation of electron–hole pairs (see e.g., Pierret, 1987, Chapter 5). The balance of electrons in the conduction band reads in integral form

$$\frac{\mathrm{d}}{\mathrm{d}t}\int_{\mathcal{P}_t} \rho n \,\mathrm{d}v = -\int_{\mathcal{P}_t} R \,\mathrm{d}v - \int_{\partial\mathcal{P}_t} \boldsymbol{\jmath}_n\cdot\mathbf{n}\,\mathrm{d}a, \tag{2.11}$$

where $\mathbf{n}$ denotes the outward unit normal to $\partial\mathcal{P}_t$. Localization of (2.11) furnishes

$$\rho\dot n = -R - \nabla\cdot\boldsymbol{\jmath}_n. \tag{2.12}$$

Similarly, denoting by $\jmath_p(\mathbf{x}, t)$ the hole current density, the local form of the balance of holes in the valence band is given by

$$\rho\dot p = -R - \nabla\cdot\boldsymbol{\jmath}_p. \tag{2.13}$$

Note that it is the same R that appears in (2.12) and (2.13). As illustrated in Fig. 1, the case $R > 0$ ($R < 0$) accounts for the transition of an electron from the conduction to the valence band (from the valence to the conduction band), i.e., a

[3] R is defined as the number of electron that *leave* the conduction band per unit time and per unit volume, which justifies the minus sign in (2.11).

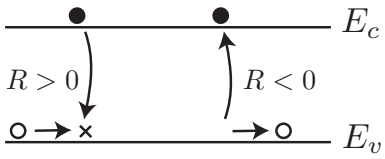

Fig. 1. Schematic of interband recombination–generation of electron–hole pairs. When $R > 0$, an electron transitions from the conduction to the valence band, where it fills a hole, thereby reducing the total number of holes in the valence band by one. Conversely, for $R < 0$, the transition of an electron to the conduction band creates a hole in the valence band.

recombination (generation) of an electron–hole pair. While in practice these transitions may involve states where electrons are located in intermediate trap levels, by using a unique term R, we consider that in the final balance of the recombination–generation processes, intermediate states are not occupied.

Finally note that the total current density of free charges appearing in Ampère's law (2.8) can be written in terms of $\boldsymbol{\jmath}_n$ and $\boldsymbol{\jmath}_p$ as

$$\boldsymbol{\jmath} = q\rho(C + p - n)\dot{\mathbf{x}} + q(\boldsymbol{\jmath}_p - \boldsymbol{\jmath}_n). \tag{2.14}$$

2.1.4. Balance of linear momentum

For the balance of linear momentum, we follow the approach in Kovetz (2000) by introducing a total Cauchy stress tensor $\boldsymbol{\sigma}(\mathbf{x}, t)$ whose related total traction $\mathbf{t} = \mathbf{n}\cdot\boldsymbol{\sigma}$ accounts for the force per unit area exerted across an elementary oriented surface $\mathbf{n}da$ by both the nearby material and the electric field. In that way, we assume the action of the electric field on matter to be completely described by surface forces distributed in the entire body, whose values are provided by a constitutive relation along with the mechanical surface tractions.

With that prospective, denoting by $\mathbf{f}(\mathbf{x}, t)$ the (purely mechanical) specific body force, the balance of linear momentum reads

$$\frac{\mathrm{d}}{\mathrm{d}t}\int_{\mathcal{P}_t} \rho\dot{\mathbf{x}}\,\mathrm{d}v = \int_{\mathcal{P}_t} \rho\mathbf{f}\,\mathrm{d}v + \int_{\partial\mathcal{P}_t} \mathbf{t}\,\mathrm{d}a. \tag{2.15}$$

Localization then yields

$$\rho\ddot{\mathbf{x}} = \nabla\cdot\boldsymbol{\sigma} + \rho\mathbf{f}. \tag{2.16}$$

2.1.5. Balance of angular momentum

Denoting by $\times$ the cross product, the balance of angular momentum of a material volume $\mathcal{P}_t$ written with respect to the origin O reads

$$\frac{\mathrm{d}}{\mathrm{d}t}\int_{\mathcal{P}_t} \mathbf{x}\times(\rho\dot{\mathbf{x}})\,\mathrm{d}v = \int_{\mathcal{P}_t} \mathbf{x}\times(\rho\mathbf{f})\,\mathrm{d}v + \int_{\partial\mathcal{P}_t} \mathbf{x}\times\mathbf{t}\,\mathrm{d}a, \tag{2.17}$$

Consistent with (2.15), all electrical contributions to the external moment are included in the surface density of moment $\mathbf{x}\times\mathbf{t}$.

By a classic derivation, applied here to the total stress tensor, one can show (see e.g., Chadwick, 1976) that (2.17) combined with (2.16) leads to the symmetry of the total Cauchy stress tensor:

$$\boldsymbol{\sigma} = \boldsymbol{\sigma}^T. \tag{2.18}$$

2.1.6. Energy balance

Let $\varepsilon(\mathbf{x}, t)$ be the total specific energy[4] (i.e., the sum of the kinetic, internal, and electrostatic energies per unit mass). Denote by

$$\mathcal{M} := \int_{\mathcal{P}_t} \rho\mathbf{f}\cdot\dot{\mathbf{x}}\,\mathrm{d}v + \int_{\partial\mathcal{P}_t} \mathbf{t}\cdot\dot{\mathbf{x}}\,\mathrm{d}a \tag{2.19}$$

the power expended by body and surface forces,

$$\mathcal{Q} := \int_{\mathcal{P}_t} \rho r\,\mathrm{d}v - \int_{\partial\mathcal{P}_t} \mathbf{q}\cdot\mathbf{n}\,\mathrm{d}a \tag{2.20}$$

the heating due to heat source $r(\mathbf{x}, t)$ and heat flux density $\mathbf{q}(\mathbf{x}, t)$,

$$\mathcal{R} := -\int_{\partial\mathcal{P}_t} [(\dot{\mathbf{x}}\times\mathbf{d})\times\mathbf{e}]\cdot\mathbf{n}\,\mathrm{d}a \tag{2.21}$$

[4] Note that in the present formulation, the potential energy of the charge densities in the electric potential φ is not included in ε. Accordingly, the power of the usual Lorentz force (that derives from φ in the absence of magnetic field) on free charges is part of the external supply: it comes as a part of the power contribution $\mathcal{R}$.

the electric energy flux density,[5] and let

$$\mathcal{S} := -\int_{\partial\mathcal{P}_t} (\mu_n \boldsymbol{\jmath}_n + \mu_p \boldsymbol{\jmath}_p)\cdot\mathbf{n}\,\mathrm{d}a \tag{2.22}$$

be the energy flow associated to free carriers, where $\mu_n(\mathbf{x}, t)$ and $\mu_p(\mathbf{x}, t)$ are the chemical potentials of electrons and holes defined as the energy carried by these two particles, respectively.[6] The energy balance applied to $\mathcal{P}_t$ reads

$$\frac{\mathrm{d}}{\mathrm{d}t}\int_{\mathcal{P}_t} \rho\varepsilon\,\mathrm{d}v = \mathcal{M} + \mathcal{Q} + \mathcal{R} + \mathcal{S}, \tag{2.23}$$

Localization delivers

$$\rho\dot{\varepsilon} = \rho\mathbf{f}\cdot\dot{\mathbf{x}} + \nabla\cdot(\boldsymbol{\sigma}\cdot\dot{\mathbf{x}}) + \rho r - \nabla\cdot\mathbf{q} - \nabla\cdot[(\dot{\mathbf{x}}\times\mathbf{d})\times\mathbf{e}] - \nabla\cdot(\mu_n\boldsymbol{\jmath}_n) - \nabla\cdot(\mu_p\boldsymbol{\jmath}_p). \tag{2.24}$$

Further, we note that the material time derivative formula applied to $\mathbf{d}$, when combined with Ampère's law (2.8), Gauss's law (2.5) and (2.14) yields

$$\dot{\mathbf{x}}\cdot\nabla\mathbf{d} = \dot{\mathbf{d}} - \frac{\partial\mathbf{d}}{\partial t} = \dot{\mathbf{d}} + (\nabla\cdot\mathbf{d})\dot{\mathbf{x}} + q(\boldsymbol{\jmath}_p - \boldsymbol{\jmath}_n), \tag{2.25}$$

which, on appeal to standard tensor identities,[7] allows us to rewrite the local flux of electric energy density as

$$-\nabla\cdot[(\dot{\mathbf{x}}\times\mathbf{d})\times\mathbf{e}] = [\dot{\mathbf{d}} + q(\boldsymbol{\jmath}_p - \boldsymbol{\jmath}_n)]\cdot\mathbf{e} + [-\mathbf{d}\mathbf{e} + (\mathbf{e}\cdot\mathbf{d})\mathbf{I}]\cdot\cdot(\dot{\mathbf{x}}\nabla), \tag{2.26}$$

where $\mathbf{I}$ is the identity rank-2 tensor. Finally, on introducing the total specific internal energy

$$u := \varepsilon - \frac{1}{2}\dot{\mathbf{x}}\cdot\dot{\mathbf{x}} \tag{2.27}$$

and using the linear momentum balance (2.16) to eliminate the power of the external body force as well as the balances (2.12) and (2.13) of free carriers, the energy balance (2.24) has the form

$$\begin{aligned}\rho\dot{u} = {}& [\boldsymbol{\sigma} - \mathbf{d}\mathbf{e} + (\mathbf{e}\cdot\mathbf{d})\mathbf{I}]\cdot\cdot(\dot{\mathbf{x}}\nabla) + \mathbf{e}\cdot\dot{\mathbf{d}} + \rho r - \nabla\cdot q \\ & - \nabla(\mu_n - q\varphi)\cdot\boldsymbol{\jmath}_n - \nabla(\mu_p + q\varphi)\cdot\boldsymbol{\jmath}_p + \rho(\mu_n\dot{n} + \mu_p\dot{p}) + (\mu_n + \mu_p)R.\end{aligned} \tag{2.28}$$

2.1.7. Entropy imbalance

Let η be the specific entropy, and denote by θ the absolute temperature. The second law of thermodynamics takes the form of the classical Clausius–Duhem inequality:

$$\frac{\mathrm{d}}{\mathrm{d}t}\int_{\mathcal{P}_t} \rho\eta\,\mathrm{d}v \geq \int_{\mathcal{P}_t} \frac{\rho r}{\theta}\,\mathrm{d}v + \int_{\partial\mathcal{P}_t} \frac{\mathbf{q}\cdot\mathbf{n}}{\theta}\,\mathrm{d}a. \tag{2.29}$$

When combined with (2.28), the local form of (2.29) takes the form

$$\begin{aligned}&\rho(\theta\dot{\eta} - \dot{u}) + [\boldsymbol{\sigma} - \mathbf{d}\mathbf{e} + (\mathbf{e}\cdot\mathbf{d})\mathbf{I}]\cdot\cdot(\dot{\mathbf{x}}\nabla) + \mathbf{e}\cdot\dot{\mathbf{d}} + \rho(\mu_n\dot{n} + \mu_p\dot{p}) \\ &\qquad - \nabla(\mu_n - q\varphi)\cdot\boldsymbol{\jmath}_n - \nabla(\mu_p + q\varphi)\cdot\boldsymbol{\jmath}_p + (\mu_n + \mu_p)R - \frac{1}{\theta}\mathbf{q}\cdot(\nabla\theta) \geq 0.\end{aligned} \tag{2.30}$$

Introducing the specific free-energy

$$\psi := u - \theta\eta - \frac{\epsilon_0}{2\rho}\mathbf{e}\cdot\mathbf{e}, \tag{2.31}$$

we can recast (2.30) as a free-energy imbalance:

$$\begin{aligned}&\rho(\dot{\psi} + \eta\dot{\theta}) - \Big[\boldsymbol{\sigma} - \mathbf{d}\mathbf{e} + \frac{\epsilon_0}{2}(\mathbf{e}\cdot\mathbf{e})\mathbf{I}\Big]\cdot\cdot(\dot{\mathbf{x}}\nabla) - \rho\mathbf{e}\cdot\dot{\mathbf{P}} - \rho(\mu_n\dot{n} + \mu_p\dot{p}) \\ &\qquad + \nabla(\mu_n - q\varphi)\cdot\boldsymbol{\jmath}_n + \nabla(\mu_p + q\varphi)\cdot\boldsymbol{\jmath}_p - (\mu_n + \mu_p)R + \frac{1}{\theta}\mathbf{q}\cdot(\nabla\theta) \leq 0.\end{aligned} \tag{2.32}$$

2.2. Constitutive relations

To complete the set of general principles, constitutive laws are needed for

$$\psi,\ \eta,\ \mathbf{e},\ \boldsymbol{\sigma},\ \mu_n,\ \mu_p,\ \boldsymbol{\jmath}_n,\ \boldsymbol{\jmath}_p,\ \mathbf{q},\ \text{and } R.$$

We assume these fields to depend on $\mathbf{F}$, $\mathbf{P}$, n, p, and θ, where $\mathbf{F}(\mathbf{x}, t)$ is the deformation gradient. Further, guided by (2.32), we assume that $\boldsymbol{\jmath}_n$ and $\boldsymbol{\jmath}_p$ depend also on $\nabla(\mu_n - q\varphi)$ and $\nabla(\mu_p + q\varphi)$, respectively, and $\mathbf{q}$ on $\nabla\theta$.

[5] The expression $(\dot{\mathbf{x}}\times\mathbf{d})\times\mathbf{e}$ for the electric energy flux density results from the specialization of the cross product $\mathcal{E}\times\mathcal{H}$ of the Galilean invariants of the magnetic and electric fields (Kovetz, 2000, Chapter 15) to situations in which the magnetic field is absent.

[6] In this way, we follow the approach of Gurtin and Vargas (1971), noting that alternative formulations are possible (Goddard, 2011; Müller, 1968). In their Remark 2.3, Gurtin and Vargas (1971) show that the different formulations are equivalent.

[7] These tensor identities are $\nabla\cdot((\dot{\mathbf{x}}\times\mathbf{d})\times\mathbf{e}) = (\nabla\times(\dot{\mathbf{x}}\times\mathbf{d}))\cdot\mathbf{e} - (\dot{\mathbf{x}}\times\mathbf{d})\cdot(\nabla\times\mathbf{e})$, $\nabla\times(\dot{\mathbf{x}}\times\mathbf{d}) = \dot{\mathbf{x}}(\nabla\cdot\mathbf{d}) - \mathbf{d}(\nabla\cdot\dot{\mathbf{x}}) + \mathbf{d}\cdot(\nabla\dot{\mathbf{x}}) - \dot{\mathbf{x}}\cdot(\nabla\mathbf{d})$.

2.2.1. Thermodynamic restrictions

We apply the Coleman–Noll procedure (Coleman and Noll, 1963), as extended by Kovetz (2000) and Gurtin and Vargas (1971) to include electrostatic and species transport, respectively, in order to place restrictions on the constitutive relations. Consequently, for a specific free energy $\psi(\mathbf{F}, \mathbf{P}, n, p, \theta)$, the free-energy imbalance (2.32) can be rewritten as

$$\left[\rho\left(\frac{\partial\psi}{\partial\mathbf{F}}\cdot\mathbf{F}^T\right)^T-\boldsymbol{\sigma}+\mathbf{de}-\frac{\epsilon_0}{2}(\mathbf{e}\cdot\mathbf{e})\mathbf{I}\right]\cdot\cdot(\dot{\mathbf{x}}\nabla)+\rho\left[\frac{\partial\psi}{\partial\mathbf{P}}-\mathbf{e}\right]\cdot\dot{\mathbf{P}}+\left[\frac{\partial\psi}{\partial n}-\mu_n\right]\rho\dot{n}+\left[\frac{\partial\psi}{\partial p}-\mu_p\right]\rho\dot{p}$$
$$+\left[\eta+\frac{\partial\psi}{\partial\theta}\right]\rho\dot{\theta}+\nabla(\mu_n-q\varphi)\cdot\mathbf{J}_n+\nabla(\mu_p+q\varphi)\cdot\mathbf{J}_p+\frac{1}{\theta}\mathbf{q}\cdot(\nabla\theta)-(\mu_n+\mu_p)R\le 0. \tag{2.33}$$

The necessary conditions for (2.33) to hold are

$$\begin{cases}\boldsymbol{\sigma}=\rho\left(\dfrac{\partial\psi}{\partial\mathbf{F}}\cdot\mathbf{F}^T\right)^T+\mathbf{de}-\dfrac{\epsilon_0}{2}(\mathbf{e}\cdot\mathbf{e})\mathbf{I},\\ \mathbf{e}=\dfrac{\partial\psi}{\partial\mathbf{P}},\quad \eta=-\dfrac{\partial\psi}{\partial\theta},\\ \mu_n=\dfrac{\partial\psi}{\partial n},\quad \mu_p=\dfrac{\partial\psi}{\partial p}.\end{cases} \tag{2.34}$$

It follows that (2.33) simplifies to the reduced dissipation inequality

$$\nabla(\mu_n-q\varphi)\cdot\mathbf{J}_n+\nabla(\mu_p+q\varphi)\cdot\mathbf{J}_p+\frac{1}{\theta}\mathbf{q}\cdot(\nabla\theta)-(\mu_n+\mu_p)R\le 0. \tag{2.35}$$

Ignoring possible cross couplings between the dissipative fluxes and the associated thermodynamic forces we postulate the following linear relations:

$$\begin{cases}\mathbf{J}_n=-n\left(\dfrac{\rho}{q}\mathbf{M}_n\right)\cdot\Big(\nabla(\mu_n-q\varphi)\Big),\\ \mathbf{J}_p=-p\left(\dfrac{\rho}{q}\mathbf{M}_p\right)\cdot\Big(\nabla(\mu_p+q\varphi)\Big),\\ \mathbf{q}=-\mathbf{K}\cdot(\nabla\theta),\end{cases} \tag{2.36}$$

where $\mathbf{M}_n(\mathbf{F}, \mathbf{P}, \theta)$ and $\mathbf{M}_p(\mathbf{F}, \mathbf{P}, \theta)$ are the positive semi-definite mobility tensors for electrons and holes, and $\mathbf{K}(\mathbf{F}, \mathbf{P}, \theta)$ is the positive semi-definite conductivity tensor. Here, the mobilities $\mathbf{M}_n$ and $\mathbf{M}_p$ are assumed independent of n and p. Further, it is physically reasonable to assume the heat flux to be independent of n and p.

These constitutive relations satisfy (2.35). The factor ρ/q in $(2.36)_{1,2}$ is such that the dimension of the mobility tensors is length square per unit potential and time, in agreement with the conventions of semiconductor physics. The terms $\mu_n - q\varphi$ and $\mu_p + q\varphi$ are the electrochemical potentials for electrons and holes, respectively.[8]

Finally, the constitutive law for the recombination–generation term R shall satisfy:

$$(\mu_n+\mu_p)R\ge 0. \tag{2.37}$$

2.2.2. Material frame indifference

In this section, we apply the principle of material frame indifference to the different constitutive laws. In particular, it explicitly shows the symmetry of $\boldsymbol{\sigma}$. To respect the principle of material frame indifference, the specific free energy $\psi(\mathbf{F}, \mathbf{P}, n, p, \theta)$ has to satisfy (Kovetz, 2000, Chapter 15; Tadmor et al., 2012, Chapter 6) the relation

$$\psi(\mathbf{F},\mathbf{P},n,p,\theta)=\psi(\mathbf{Q}\cdot\mathbf{F},\mathbf{Q}\cdot\mathbf{P},n,p,\theta), \tag{2.38}$$

for any proper orthogonal tensor $\mathbf{Q}$. Using the polar decomposition $\mathbf{F}=\mathbf{R}\cdot\mathbf{U}$ and choosing $\mathbf{Q}=\mathbf{R}^T=\mathbf{U}^{-1}\cdot\mathbf{F}^T$ we obtain:

$$\psi(\mathbf{F},\mathbf{P},n,p,\theta)=\psi(\mathbf{U},\mathbf{U}^{-1}\cdot\mathbf{F}^T\cdot\mathbf{P},n,p,\theta). \tag{2.39}$$

It follows that ψ can be expressed as a function of $\mathbf{U}, \mathbf{F}^T\cdot\mathbf{P}, n, p, \theta$ or equivalently as a function of the same set of variable with $\mathbf{C}=\mathbf{F}^T\cdot\mathbf{F}=\mathbf{U}^2$ instead of $\mathbf{U}$. Using the form

$$\psi=\widehat{\psi}(\mathbf{C},\mathbf{F}^T\cdot\mathbf{P},n,p,\theta), \tag{2.40}$$

the free-energy automatically satisfies (2.38) for any proper orthogonal tensor $\mathbf{Q}$. The original function $\psi(\mathbf{F}, \mathbf{P}, n, p, \theta)$ can be written in terms of the new function $\widehat{\psi}(\mathbf{C}, \mathbf{F}^T\cdot\mathbf{P}, n, p, \theta)$:

$$\psi(\mathbf{F},\mathbf{P},n,p,\theta)=\widehat{\psi}(\mathbf{C},\mathbf{F}^T\cdot\mathbf{P},n,p,\theta). \tag{2.41}$$

[8] In parts of the physics literature, $\mu_n - q\varphi$ and $\mu_p + q\varphi$ are called the *total chemical potentials*, whereas μ_n and μ_p are referred to as the *internal chemical potentials*. In the semiconductor literature, $\mu_n - q\varphi$ is the quasi-Fermi level of electrons, while $\mu_p + q\varphi$ corresponds to the opposite of the quasi-Fermi level of holes (see Kittel and Kroemer, 1980, Chapter 13).

With the purpose of establishing the symmetry of the total Cauchy stress defined by (2.34) we derive from (2.41) the identities

$$\begin{cases} \dfrac{\partial \psi}{\partial \mathbf{F}} = 2\mathbf{F}\cdot\dfrac{\partial \widehat{\psi}}{\partial \mathbf{C}} + \mathbf{P}\cdot\dfrac{\partial \widehat{\psi}}{\partial (\mathbf{F}^T\cdot\mathbf{P})}, \\ \dfrac{\partial \psi}{\partial \mathbf{P}} = \dfrac{\partial \widehat{\psi}}{\partial (\mathbf{F}^T\cdot\mathbf{P})}\cdot\mathbf{F}^T = \mathbf{F}\cdot\dfrac{\partial \widehat{\psi}}{\partial (\mathbf{F}^T\cdot\mathbf{P})}. \end{cases} \tag{2.42}$$

In view of these identities, we rewrite (2.34) in terms of the function $\widehat{\psi}$:

$$\boldsymbol{\sigma} = \rho\Big(2\mathbf{F}\cdot\frac{\partial \widehat{\psi}}{\partial \mathbf{C}}\cdot\mathbf{F}^T + \mathbf{P}\mathbf{e} + \mathbf{e}\mathbf{P}\Big) + \epsilon_0\Big(\mathbf{e}\mathbf{e} - \frac{1}{2}(\mathbf{e}\cdot\mathbf{e})\mathbf{I}\Big) = \boldsymbol{\sigma}^T, \tag{2.43}$$

which shows the symmetry of $\boldsymbol{\sigma}$.

As a result of the frame indifference of the specific free energy $\widehat{\psi}$, the fields $\boldsymbol{\sigma}$, $\mathbf{e}$, $\boldsymbol{\eta}$, μ_n and μ_p given by (2.43),

$$\mathbf{e} = \mathbf{F}\cdot\frac{\partial \widehat{\psi}}{\partial (\mathbf{F}^T\cdot\mathbf{P})}, \quad \eta = -\frac{\partial \widehat{\psi}}{\partial \theta}, \quad \mu_n = \frac{\partial \widehat{\psi}}{\partial n}, \quad \text{and} \quad \mu_p = \frac{\partial \widehat{\psi}}{\partial p}, \tag{2.44}$$

are also frame indifferent, i.e., they automatically satisfy for every proper orthogonal tensor $\mathbf{Q}$ the following relations:

$$\begin{cases} \boldsymbol{\sigma}\big(\mathbf{Q}\cdot\mathbf{F}, \mathbf{Q}\cdot\mathbf{P}, n, \theta\big) = \mathbf{Q}\cdot\boldsymbol{\sigma}\big(\mathbf{F}, \mathbf{P}, n, \theta\big)\cdot\mathbf{Q}^T, & \mathbf{e}\big(\mathbf{Q}\cdot\mathbf{F}, \mathbf{Q}\cdot\mathbf{P}, n, \theta\big) = \mathbf{Q}\cdot\mathbf{e}\big(\mathbf{F}, \mathbf{P}, n, \theta\big), \\ \eta\big(\mathbf{Q}\cdot\mathbf{F}, \mathbf{Q}\cdot\mathbf{P}, n, \theta\big) = \eta\big(\mathbf{F}, \mathbf{P}, n, \theta\big), & \mu_n\big(\mathbf{Q}\cdot\mathbf{F}, \mathbf{Q}\cdot\mathbf{P}, n, \theta\big) = \mu_n\big(\mathbf{F}, \mathbf{P}, n, \theta\big), \\ \mu_p\big(\mathbf{Q}\cdot\mathbf{F}, \mathbf{Q}\cdot\mathbf{P}, n, \theta\big) = \mu_p\big(\mathbf{F}, \mathbf{P}, n, \theta\big). \end{cases} \tag{2.45}$$

In addition, we require the electron, hole and heat current densities to be frame indifferent, i.e.,

$$\begin{cases} \boldsymbol{\jmath}_n\big(\mathbf{Q}\cdot\mathbf{F}, \mathbf{Q}\cdot\mathbf{P}, n, \theta, \mathbf{Q}\cdot\nabla(\mu_n - q\varphi)\big) = \mathbf{Q}\boldsymbol{\jmath}_n\big(\mathbf{F}, \mathbf{P}, n, \theta, \nabla(\mu_n - q\varphi)\big), \\ \boldsymbol{\jmath}_p\big(\mathbf{Q}\cdot\mathbf{F}, \mathbf{Q}\cdot\mathbf{P}, p, \theta, \mathbf{Q}\cdot\nabla(\mu_p + q\varphi)\big) = \mathbf{Q}\boldsymbol{\jmath}_p\big(\mathbf{F}, \mathbf{P}, p, \theta, \nabla(\mu_p + q\varphi)\big), \\ \mathbf{q}\big(\mathbf{Q}\cdot\mathbf{F}, \mathbf{Q}\cdot\mathbf{P}, \theta, \mathbf{Q}\cdot\nabla\theta\big) = \mathbf{Q}\cdot\mathbf{q}\big(\mathbf{F}, \mathbf{P}, n, \theta, \nabla\theta\big). \end{cases} \tag{2.46}$$

Given (2.36), necessary and sufficient conditions for (2.46) to hold are

$$\begin{cases} \mathbf{M}_n(\mathbf{Q}\cdot\mathbf{F}, \mathbf{Q}\cdot\mathbf{P}, \theta) = \mathbf{Q}\cdot\mathbf{M}_n(\mathbf{F}, \mathbf{P}, \theta)\cdot\mathbf{Q}^T, \\ \mathbf{M}_p(\mathbf{Q}\cdot\mathbf{F}, \mathbf{Q}\cdot\mathbf{P}, \theta) = \mathbf{Q}\cdot\mathbf{M}_p(\mathbf{F}, \mathbf{P}, \theta)\cdot\mathbf{Q}^T, \\ \mathbf{K}(\mathbf{Q}\cdot\mathbf{F}, \mathbf{Q}\cdot\mathbf{P}, \theta) = \mathbf{Q}\cdot\mathbf{K}(\mathbf{F}, \mathbf{P}, \theta)\cdot\mathbf{Q}^T. \end{cases} \tag{2.47}$$

2.3. Crystalline semiconductors

Since crystalline semiconductors are brittle materials, we specialize the above finite-deformation theory to small strains. In doing so, we restrict our attention to isothermal processes.

2.3.1. Small-strain assumption

Under the above assumptions, the deformation is described by the small-strain tensor

$$\boldsymbol{\varepsilon} = \frac{1}{2}\big(\mathbf{u}\nabla + \nabla\mathbf{u}\big), \tag{2.48}$$

where $\mathbf{u} = \mathbf{x} - \mathbf{X}$ is the displacement field. The condition

$$\|\boldsymbol{\varepsilon}\| = (\boldsymbol{\varepsilon} : \boldsymbol{\varepsilon})^{1/2} \ll 1 \tag{2.49}$$

is satisfied since strains remain less than 10^{-2} in crystalline materials. At first-order in $\boldsymbol{\varepsilon}$, (2.43) is approximated by

$$\boldsymbol{\sigma}(\boldsymbol{\varepsilon}, \mathbf{P}, n, p) = \rho\Big(\frac{\partial \widehat{\psi}}{\partial \boldsymbol{\varepsilon}} + \mathbf{P}\mathbf{e} + \mathbf{e}\mathbf{P}\Big) + \epsilon_0\Big(\mathbf{e}\mathbf{e} - \frac{1}{2}(\mathbf{e}\cdot\mathbf{e})\mathbf{I}\Big). \tag{2.50}$$

In accordance with the small-strain assumption, changes of volume are neglected and ρ is taken to be constant.

2.3.2. Choice of a free energy

We postulate an additive decomposition of the specific free energy into mechanical, electrostatic and electronic components:

$$\widehat{\psi}(\boldsymbol{\varepsilon}, \mathbf{P}, n, p) := \widehat{\psi}_{mech}(\boldsymbol{\varepsilon}) + \widehat{\psi}_{elecs}(\mathbf{P}) + \widehat{\psi}_{elecn}(\boldsymbol{\varepsilon}, n, p). \tag{2.51}$$

This additive decomposition of the free energy is natural given that the semiconductor under investigation is assumed to be a centrosymetric crystal, i.e., a material that does not exhibit piezoelectricity. For a non-centrosymmetric semiconductor

with piezoelectric behavior, an additional coupling term between strain and polarization of the form $\widehat{\psi}_{piezo}(\boldsymbol{\varepsilon}, \mathbf{P}) = \boldsymbol{\varepsilon} : \mathbf{N}\cdot\mathbf{P}$, with $\mathbf{N}$ a constitutive rank-3 tensor, should be added to the right hand side of (2.51).

One feature that distinguishes (2.51) from exisiting constitutive models (e.g., Xiao and Bhattacharya, 2008) is the dependence of the electronic component $\widehat{\psi}_{elecn}$ on strain. Specifically, this dependence accounts for the strain-induced changes of the electronic band structure. Further, a more general constitutive relation for the free energy of a deformable semiconductor would allow for a dependence of $\widehat{\psi}_{elecn}$ on polarization. However in the absence of a strong electric field, we expect this dependence to be negligible.[9] Finally, in the small-strain regime, the permittivity ϵ_r of the material can be assumed constant. Hence, $\widehat{\psi}_{elecs}$ does not depend on strain.

For a linearly elastic material, the mechanical part is given by

$$\widehat{\psi}_{mech}(\boldsymbol{\varepsilon}) := \frac{1}{2\rho}\boldsymbol{\varepsilon} : \mathbf{c} : \boldsymbol{\varepsilon}, \tag{2.52}$$

with $\mathbf{c}$ the elasticity tensor of the material.

The electrostatic part of the free energy $\widehat{\psi}_{elecs}$ corresponds to the free energy of a linear isotropic dielectric of permittivity ϵ_r:

$$\widehat{\psi}_{elecs}(\mathbf{P}) := \frac{\rho}{2(\epsilon_r - \epsilon_0)}\mathbf{P}\cdot\mathbf{P}. \tag{2.53}$$

The electronic component $\widehat{\psi}_{elecn}$ of the free energy is related to the densities of electrons and holes. Assuming that the electron and hole gases are in local equilibrium in the conduction and valence bands independently, the expression of the free energy is given by statistical physics (see e.g., Kittel and Kroemer, 1980). Denoting by $E_c(\boldsymbol{\varepsilon})$ and $E_v(\varepsilon)$ the band edge energy levels of the conduction and valence bands *in the absence of electric potential* ($\varphi = 0$),[10] and by $N_c(\boldsymbol{\varepsilon})$ and $N_v(\varepsilon)$ the effective densities of state of the conduction and valence bands respectively (in number of states per unit mass), the specific free energy of the two gases reads[11]

$$\widehat{\psi}_{elecn}(\boldsymbol{\varepsilon}, n, p) := n\left[k\theta\left(\ln\left(\frac{n}{N_c(\boldsymbol{\varepsilon})}\right) - 1\right) + E_c(\boldsymbol{\varepsilon})\right] + p\left[k\theta\left(\ln\left(\frac{p}{N_v(\boldsymbol{\varepsilon})}\right) - 1\right) - E_v(\boldsymbol{\varepsilon})\right], \tag{2.54}$$

where k is the Boltzmann constant. The dependence of E_c, E_v, N_c and N_v on $\boldsymbol{\varepsilon}$ is due to the fact that the band structure of a semiconductor results from its atomic lattice configuration, itself modified by strain. This dependence have been investigated in the solid-state physics literature as discussed in Section 1.

By (2.34) and (2.51), we have:

$$\begin{cases} \boldsymbol{\sigma}(\boldsymbol{\varepsilon}, \mathbf{P}, n, p) = \underbrace{\mathbf{c} : \boldsymbol{\varepsilon}}_{\boldsymbol{\sigma}_{mech}} + \underbrace{\rho n\left(-k\theta\dfrac{\partial \ln(N_c)}{\partial \boldsymbol{\varepsilon}} + \dfrac{\partial E_c}{\partial \boldsymbol{\varepsilon}}\right) + \rho p\left(-k\theta\dfrac{\partial \ln(N_v)}{\partial \boldsymbol{\varepsilon}} - \dfrac{\partial E_v}{\partial \boldsymbol{\varepsilon}}\right)}_{\boldsymbol{\sigma}_{elecn}} \\ \qquad\qquad + \underbrace{\rho\Big(\mathbf{Pe} + \mathbf{eP}\Big) + \epsilon_0\Big(\mathbf{ee} - \frac{1}{2}(\mathbf{e}\cdot\mathbf{e})\mathbf{I}\Big)}_{\boldsymbol{\sigma}_{maxw}}, \\ \mathbf{e}(\mathbf{P}) = \dfrac{\rho\mathbf{P}}{\epsilon_r - \epsilon_0}, \\ \mu_n(\boldsymbol{\varepsilon}, n) = E_c(\boldsymbol{\varepsilon}) + k\theta\ln\left(\dfrac{n}{N_c(\boldsymbol{\varepsilon})}\right), \\ \mu_p(\boldsymbol{\varepsilon}, p) = -E_v(\boldsymbol{\varepsilon}) + k\theta\ln\left(\dfrac{p}{N_v(\boldsymbol{\varepsilon})}\right). \end{cases} \tag{2.55}$$

Note that the total stress tensor $\boldsymbol{\sigma}$ not only consists of a purely mechanical component ($\boldsymbol{\sigma}_{mech}$) and a Maxwell component ($\boldsymbol{\sigma}_{maxw}$) but contains also an electronic contribution ($\boldsymbol{\sigma}_{elecn}$) which depends on electron and hole densities. As seen in $(2.55)_1$, the dependence of $\widehat{\psi}_{elecn}$ on strain results in an *electronic* contribution to the stress tensor, one that has not been accounted for previously. Regardless of the specific form of $\boldsymbol{\sigma}_{elecn}$, which follows from the constitutive assumptions (2.51) and (2.54), the existence of an electronic stress is the consequence of the dependence on strain of the effective densities of states as well as the energy levels of the valence and conduction bands.

[9] The transport of electrons and holes is nonetheless related to polarization through the gradient of the electric potential as can be seen in the derivation of the current-density relations $(2.55)_2$ and (2.56).

[10] Note that with this definition of E_c and E_v, the electrostatic potential energy of free charges does not appear in the free energy. This is consistent with our definition of the total energy which does not include the electrostatic potential energy of free charges (see footnote Section 2.1.6).

[11] The constitutive relation (2.54) corresponds to the free energy of an ideal gas of electrons and holes. It is valid for non-degenerate semiconductors, i.e., semiconductors whose free-carrier concentration is not to high, which is the case for most electronic devices. An extension of our model to degenerate semiconductors would require replacing (2.54) with the free energy of a Fermi gas of electrons and holes.

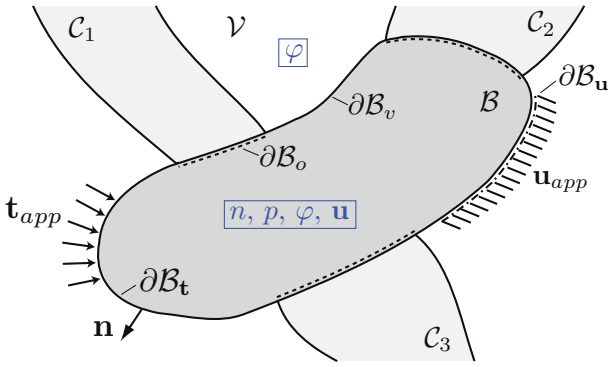

Fig. 2. Schematic of the boundary-value problem of a deformable semiconductor in contact with three electrodes.

In view of the constitutive relations $(2.55)_{3,4}$ for the chemical potentials, we rewrite $(2.36)_{1,2}$ in the form of generalized current-density relations:

$$\begin{cases} \boldsymbol{\jmath}_n = -k\theta\Big(\dfrac{\rho}{q}\mathbf{M}_n(\boldsymbol{\varepsilon})\Big)\cdot\nabla n + n\Big(\dfrac{\rho}{q}\mathbf{M}_n(\boldsymbol{\varepsilon})\Big)\cdot\Big[q\nabla\varphi - \nabla E_c(\boldsymbol{\varepsilon}) + k\theta\nabla\big(\ln(N_c(\boldsymbol{\varepsilon}))\big)\Big], \\ \boldsymbol{\jmath}_p = -k\theta\Big(\dfrac{\rho}{q}\mathbf{M}_p(\boldsymbol{\varepsilon})\Big)\cdot\nabla p + p\Big(\dfrac{\rho}{q}\mathbf{M}_p(\boldsymbol{\varepsilon})\Big)\cdot\Big[-q\nabla\varphi + \nabla E_v(\boldsymbol{\varepsilon}) + k\theta\nabla\big(\ln(N_v(\boldsymbol{\varepsilon}))\big)\Big]. \end{cases} \tag{2.56}$$

We note that Eq. (2.56) appears in the physics literature pertaining to the transport of electrons and holes in nonuniform semiconductors, where they are derived from Boltzmann transport equation (see Manku and Nathan, 1993; Marshak and Vliet, 1984; Marshak and van Vliet, 1978 and also Nelson, 2003, Chapter 3; Fonash, 2012, Chapter 2).

2.3.3. Recombination–generation

In the absence of photogeneration, the dominant mechanism of recombination–generation of electrons and holes in indirect band-gap semiconductors (such as silicon) is via bulk traps (Pierret, 1987; Sze and Ng, 2006). With the usual approximation that effective recombination–generation centers are traps lying near the mid-gap, the transition rate is described by the simplified Read–Shockley–Hall model (Pierret, 1987, Chapter 5):

$$R(n, p, \boldsymbol{\varepsilon}) = \frac{\rho(pn - n_i^2(\boldsymbol{\varepsilon}))}{\tau_p(n + n_i(\boldsymbol{\varepsilon})) + \tau_n(p + n_i(\boldsymbol{\varepsilon}))}, \tag{2.57}$$

where

$$n_i(\boldsymbol{\varepsilon}) = \sqrt{N_c(\boldsymbol{\varepsilon})N_v(\boldsymbol{\varepsilon})}\exp\left(\frac{-(E_c(\boldsymbol{\varepsilon}) - E_v(\boldsymbol{\varepsilon}))}{2k\theta}\right), \tag{2.58}$$

is the intrinsic concentration of electrons and holes and τ_n and τ_p are two positive constants interpreted as the electron and hole lifetimes, respectively.

To check the thermodynamic consistency of (2.57), we invert $(2.55)_{3,4}$ to express n and p as functions of μ_n and μ_p, and rewrite the numerator of R:

$$\rho(pn - n_i^2) = \rho N_c N_v \exp\left(\frac{-(E_c - E_v)}{k\theta}\right)\Big(\exp\big(\mu_n + \mu_p\big) - 1\Big). \tag{2.59}$$

It follows that $R(\mu_n + \mu_p)$ has the sign of $\big(\mu_n + \mu_p\big)\big(\exp\big(\mu_n + \mu_p\big) - 1\big)$ which is positive for all μ_n and μ_p as required by (2.37).

2.3.4. Summary of the governing equations for a deformable semiconductor

At this point, it is useful to summarize the governing equations for the boundary value problem of a deformable semiconductor. Since strains in a crystalline semiconductor are small, the problem is written in the reference configuration of the semiconductor $\mathcal{B}$. The unknown fields are: n, p and $\boldsymbol{u}$ inside the semiconductor, while the electric potential φ has to be determined for the entire space $\mathbb{R}^3$.

Field equations: For simplicity, it is assumed that the deformable semiconductor is either in contact with a conductor (electrode) or surrounded by free space. As depicted in Fig. 2, the deformable semiconductor is in contact with N conductors occupying disjoined regions $\mathcal{C}_i$ with $i = 1 \dots N$. Since the electric field vanishes inside a conductor, φ is constant in each $\mathcal{C}_i$. The surrounding free space is $\mathcal{V} := \mathbb{R}^3 \setminus \{\mathcal{B} \cup \mathcal{C}_1 \cup \cdots \cup \mathcal{C}_N\}$, where the electric potential φ must also be computed. The field

equations are

$$\begin{cases} \epsilon_r \Delta\varphi = q\rho(n-p-C), \\ \rho\dot{n} = -R - \nabla\cdot\boldsymbol{\jmath}_n, \\ \rho\dot{p} = -R - \nabla\cdot\boldsymbol{\jmath}_p, \\ \rho\ddot{\mathbf{u}} = \nabla\cdot\boldsymbol{\sigma} + \rho\mathbf{f}, \end{cases} \quad \text{in } \mathcal{B}, \tag{2.60}$$

where

$$\begin{cases} \boldsymbol{\jmath}_n = -k\theta\Big(\dfrac{\rho}{q}\mathbf{M}_n(\boldsymbol{\varepsilon})\Big)\cdot\nabla n + n\Big(\dfrac{\rho}{q}\mathbf{M}_n(\boldsymbol{\varepsilon})\Big)\cdot\Big[q\nabla\varphi - \nabla E_c(\boldsymbol{\varepsilon}) + k\theta\nabla\Big(\ln(N_c(\boldsymbol{\varepsilon}))\Big)\Big], \\ \boldsymbol{\jmath}_p = -k\theta\Big(\dfrac{\rho}{q}\mathbf{M}_p(\boldsymbol{\varepsilon})\Big)\cdot\nabla p + p\Big(\dfrac{\rho}{q}\mathbf{M}_p(\boldsymbol{\varepsilon})\Big)\cdot\Big[-q\nabla\varphi + \nabla E_v(\boldsymbol{\varepsilon}) + k\theta\nabla\Big(\ln(N_v(\boldsymbol{\varepsilon}))\Big)\Big], \\ R = \dfrac{\rho(pn - n_i^2(\boldsymbol{\varepsilon}))}{\tau_p(n+n_i(\boldsymbol{\varepsilon})) + \tau_n(p+n_i(\boldsymbol{\varepsilon}))}, \\ \boldsymbol{\sigma} = \mathbf{c}:\boldsymbol{\varepsilon} + \rho n\Big(-k\theta\dfrac{\partial\ln(N_c)}{\partial\boldsymbol{\varepsilon}} + \dfrac{\partial E_c}{\partial\boldsymbol{\varepsilon}}\Big) + \rho p\Big(-k\theta\dfrac{\partial\ln(N_v)}{\partial\boldsymbol{\varepsilon}} - \dfrac{\partial E_v}{\partial\boldsymbol{\varepsilon}}\Big) \\ \qquad\qquad + (2\epsilon_r - \epsilon_0)(\nabla\varphi)(\nabla\varphi) - \dfrac{\epsilon_0}{2}\big(\nabla\varphi\cdot\nabla\varphi\big)\mathbf{I}, \\ \boldsymbol{\varepsilon} = \dfrac{1}{2}\big(\mathbf{u}\nabla + \nabla\mathbf{u}\big), \end{cases} \tag{2.61}$$

along with Laplace's equation for the electric potential in free space:

$$\Delta\varphi = 0 \quad \text{in } \mathcal{V}. \tag{2.62}$$

The boundary $\partial\mathcal{B}$ is split as follows. With respect to the electronic part, let $\partial\mathcal{B}_o$ be the union of contact surfaces with the conductors $\mathcal{C}_i$ and $\partial\mathcal{B}_v$ the interfaces with the free space $\mathcal{V}$. With respect to mechanics, we distinguish between $\partial\mathcal{B}_{\mathbf{u}}$ where a displacement $\mathbf{u}_{app}$ is prescribed and $\partial\mathcal{B}_{\mathbf{t}}$ where an external mechanical traction $\mathbf{t}_{app}$ is applied. From these definitions follows that $\partial\mathcal{B}_o \cup \partial\mathcal{B}_v = \partial\mathcal{B}$ and $\partial\mathcal{B}_{\mathbf{u}} \cup \partial\mathcal{B}_{\mathbf{t}} = \partial\mathcal{B}$. Depending on the problem, the electronic and mechanical parts of the boundary can overlap.

Electronic boundary conditions: Assuming voltage-controlled ohmic contacts with the conductors, conditions are (Selberherr, 1984):

$$\begin{cases} \varphi = \varphi_{bin} + \varphi_{app}, \\ n - p - C = 0 \\ np - n_i^2 = 0, \end{cases} \quad \text{on } \partial\mathcal{B}_o, \tag{2.63}$$

where φ_{bin} is the built-in potential and φ_{app} the externally applied bias. The built-in potential is obtained by computing the steady-state solution of (2.60) in the mechanical equilibrium case and in the absence of externally applied bias ($\varphi_{app} = 0$ on $\partial\mathcal{B}_o$). Further, $(2.63)_2$ and $(2.63)_3$ correspond to the common assumptions of vanishing space charge and thermal equilibrium (absence of surface recombination) at ohmic contacts (Selberherr, 1984). Their resolution yields Dirichlet boundary conditions for the concentrations of electrons and holes.

Along the interface $\partial\mathcal{B}_v$ with free space, jump conditions for the electric potential φ and the normal component of its gradient must be satisfied. Moreover, in the absence of surface recombination, the flows of electrons and holes must vanish at $\partial\mathcal{B}_v$. We therefore have

$$\begin{cases} [\![\epsilon\nabla\varphi]\!]\cdot\mathbf{n} = 0, \\ [\![\varphi]\!] = 0, \\ \boldsymbol{\jmath}_n\cdot\mathbf{n} = 0, \\ \boldsymbol{\jmath}_p\cdot\mathbf{n} = 0. \end{cases} \quad \text{on } \partial\mathcal{B}_v, \tag{2.64}$$

where $\mathbf{n}$ is the unit outward normal to $\partial\mathcal{B}_v$ and $[\![f]\!] := f_{vac} - f_{sem}$ denotes the jump of the field quantity f at the interface.[12]

Mechanical boundary conditions: Denoting by $\mathbf{u}_{app}$ the prescribed displacement on $\partial\mathcal{B}_{\mathbf{u}}$, the displacement boundary condition reads

$$\mathbf{u} = \mathbf{u}_{app} \quad \text{on } \partial\mathcal{B}_{\mathbf{u}}. \tag{2.65}$$

Finally, on $\partial\mathcal{B}_{\mathbf{t}}$ where a mechanical traction is prescribed, the localization of linear momentum balance (2.15) on a volume surrounding $\partial\mathcal{B}_{\mathbf{t}}$ yields[13]

$$\mathbf{n}\cdot[\![\boldsymbol{\sigma}]\!] = \mathbf{t}_{app} \quad \text{on } \partial\mathcal{B}_{\mathbf{t}}. \tag{2.66}$$

[12] Note that in the absence of interface charge, $(2.64)_1$ results from the localization at the semiconductor/free space interface of the integral forms of Gauss's law (2.5).

[13] Note that in free space, the total stress tensor reduces to Maxwell stress $\boldsymbol{\sigma} = \epsilon_0[(\nabla\varphi)(\nabla\varphi)\big|_{vac} - (1/2)\big(\nabla\varphi\cdot\nabla\varphi\big)\big|_{vac}\mathbf{I}]$.

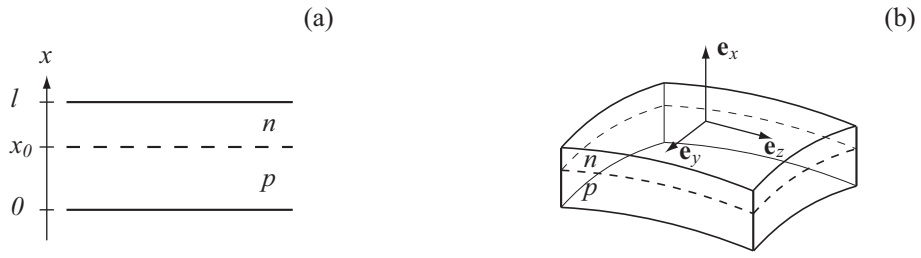

Fig. 3. Schematic of an in plane $p-n$ junction. (a) Reference configuration $\mathcal{B}_0$, n and p denote the n-doped and p-doped regions, respectively. (b) Deformed configuration bent about the directions $\mathbf{e}_y$ and $\mathbf{e}_z$.

2.3.5. Stress in silicon

Here, we consider silicon to compare the relative magnitudes of the different components of the total stress tensor $(2.55)_1$. We show that, in the case of non-degenerate[14] silicon, the influence of electric field and electronic distribution on the stress is negligible, which reduces the couplings to the influence of strain on the electronic transport. However, in the high doping regime (e.g., in degenerate silicon), the new electronic contribution to the stress could become important.

We first evaluate the purely mechanical part of the stress $\boldsymbol{\sigma}_{mech}$ from $(2.55)_1$. Given the Young modulus of silicon ($E = 130\,\text{GPa}$) and considering that the operating strains range between 10^{-4} and 10^{-2}, the corresponding mechanical contribution to stress ranges from 10 MPa to 1 GPa.

To compute an upper bound of the electronic contribution $\boldsymbol{\sigma}_{elecn}$ to the stress, we consider the maximum carrier density in non-degenerate semiconductors ($10^{18}\,\text{atoms/cm}^3$) and the typical energetic variations per unit strain of the conduction and valence band levels and effective densities of states at room temperature ($1-3\,\text{eV}$) (cf. Appendix A). Thus, the electronic contribution to stress is no more than 0.5 MPa.

The last contribution is the Maxwell stress $\boldsymbol{\sigma}_{maxw}$ related to the electric field and polarization. As an upper bound again, we consider the maximum electric field observed at the $p-n$ interface in the space charge region of a highly doped $p-n$ junction: $10^7\,\text{V/m}$. With the dielectric constant of silicon $\epsilon_r = 11.9\epsilon_0$, we obtain that the Maxwell contribution to stress does not exceed 100 kPa.

We observe that the electronic and Maxwell contributions to the stress are at least one order of magnitude lower than the smallest operating purely mechanical stress. As a result, for non-degenerate silicon, there is no significant influence of the electronics and the electric field on the mechanics, thus the mechanical problem can be solved independently of the electronic state.

We remark however that for high doping such as $5\times10^{19}\,\text{atoms/cm}^3$ the electronic contribution to stress is of the order of 25 MPa, which is significant. Besides, the Young modulus of a semiconductor (which is nothing but the derivative of $\boldsymbol{\sigma}$ with respect to $\boldsymbol{\varepsilon}$ evaluated at zero strain) is expected to depend on the electron and hole concentrations in proportion to the second derivative of the band energy levels and density of states with $\boldsymbol{\varepsilon}$. This could contribute to the unusual values of the Young modulus measured for heavily doped semiconductors which have so far been explained by the changes induced by the presence of the dopant nuclei (Ding et al., 1990; Ericson and Schweitz, 1990; Najafi and Suzuki, 1989).

3. Bending of a $p-n$ junction

In this section, we make use of the governing field equations derived in Section 2 to compute $\jmath(V)$, the *current–voltage characteristic* (or *characteristic* for short), of a $p-n$ junction undergoing nonuniform strains as a result of the bending of the device. In Section 3.1 the inherently three-dimensional problem is reduced to its one-dimensional counterpart. By means of asymptotics, $\jmath(V)$ is computed in Section 3.2 as a function of the applied strain and curvature. Finally, the result of Section 3.2 is applied in Section 3.3 to compute the strain-induced changes in the characteristic of a typical monocrystalline silicon solar cell subjected to bending. Changes in $\jmath(V)$ of the order 20% are predicted for strains of about 0.2%.

3.1. Motivation and problem setting

We consider a $p-n$ junction parallel to the mid-plane of a plate made of a crystalline semiconductor, see Fig. 3(a), whose Helmholtz free-energy is given by (2.51). The simplifications derived in Section 2.3.5 for silicon remain valid for the material considered. Indeed, this is likely to be the case for the centro-symmetric crystalline semiconductors used in practical applications.

The junction occupies the space between the planes $x = 0$ and $x = l$ with the $p-n$ interface located at the plane $x = x_0$. Without loss of generality, we consider that the p region contains only acceptors while the n region contains only donors.

[14] In practice, a semiconductor is non-degenerate when its dopant concentrations are not too high and becomes degenerate when the doping overpass some limit, see e.g., Sze and Ng (2006).

Hence, (2.1) specializes to

$$C(x,y,z)=\begin{cases}-N_a & \text{for } x\in(0,x_0),\\ N_d & \text{for } x\in(x_0,l),\end{cases} \tag{3.1}$$

where N_a and N_d are the constant numbers of acceptors and donors per unit mass in the regions p and n, respectively.

The electric current $\boldsymbol{J}:=q(\boldsymbol{J}_p-\boldsymbol{J}_n)$, which results from the external voltage V applied between the surfaces $x=0$ and $x=l$, is affected by the bending of the junction. Existing studies of the strain effect on the $p-n$ junction (piezojunction effect) consider *uniform strain* whose effect on the electric current is computed by simply substituting, in the classical current–voltage characteristic of Shockley, the values under strain of the electronic parameters. In contrast, the bending of the device results in *nonuniform strains* across the junction, thus modifying the boundary-value problem whose solution is used to compute the current–voltage characteristic, as detailed in what follows.

3.1.1. Strain field

We start by describing the equilibrium strain field in the junction. The plate is bent about the directions $\mathbf{e}_y$ and $\mathbf{e}_z$, so that the yy- and zz-components of the small-strain tensor are given by

$$\begin{cases}\varepsilon_{yy}(x,y,z)=\kappa_y(x-x_0)+\varepsilon^0_{yy},\\ \varepsilon_{zz}(x,y,z)=\kappa_z(x-x_0)+\varepsilon^0_{zz},\end{cases} \tag{3.2}$$

where κ_y and κ_z are the curvatures associated with the principal strain directions $\mathbf{e}_y$ and $\mathbf{e}_z$, and ε^0_{yy} and ε^0_{zz} are the strain components at $x=x_0$. Let $\kappa:=max(\kappa_y,\kappa_z)$ be a characteristic curvature. We introduce the dimensionless coefficients

$$\alpha_y:=\frac{\kappa_y}{\kappa},\qquad \alpha_z:=\frac{\kappa_z}{\kappa}. \tag{3.3}$$

Although the displacements and rotations may be large, the strains remain small. The surfaces $x=\texttt{constant}$ that are planar in the reference configuration are mapped into curved surfaces in the deformed configuration. However, these surfaces can be locally approximated by their tangent planes and the problem reduces to a planar one. Since we neglect the influence of the boundaries in the directions y and z, the problem is invariant under y- and z-translations. In addition, we consider the stationary problem in the absence of body force. In view of the simplifications introduced in Section 2.3.5, the total stress is approximated by the mechanical part of the stress,

$$\boldsymbol{\sigma}=\mathbf{c}:\boldsymbol{\varepsilon}, \tag{3.4}$$

where $\mathbf{c}$ is the elasticity tensor of the semiconductor. For cubic symmetry crystalline semiconductors, such as silicon, and assuming that the symmetry axes align with the coordinates, the mechanical equilibrium (2.16) combined with the traction-free boundary conditions on the surfaces $x=0$ and $x=l$, yields $\sigma_{xx}=\sigma_{xy}=\sigma_{xz}=0$ everywhere in the junction. It follows from (3.4) that

$$\varepsilon_{xx}(x,y,z)=-\frac{c_{xxyy}}{c_{xxxx}}\Big[\varepsilon_{yy}(x,y,z)+\varepsilon_{zz}(x,y,z)\Big]=-\frac{c_{xxyy}}{c_{xxxx}}\Big[\kappa(\alpha_y+\alpha_z)(x-x_0)+\varepsilon^0_{yy}+\varepsilon^0_{zz}\Big], \tag{3.5}$$

and the shear components of $\boldsymbol{\varepsilon}$ vanish.

3.1.2. Strain dependence of the electronic parameters

Next, we present the dependence of the electronic parameters E_c, E_v, N_c, N_v, $\mathbf{M}_n$ and $\mathbf{M}_p$ on $\boldsymbol{\varepsilon}$ and deduce their spatial variation in x using the strain field Eqs. (3.2) and (3.5). In view of the small-strain assumption, linear relationships in the small-strain tensor $\boldsymbol{\varepsilon}$ are considered. The strain dependence of the band edges E_c and E_v and of the effective densities of state N_c and N_v of the conduction and valence bands is given by:[15]

$$\begin{cases}E_c(\boldsymbol{\varepsilon})=E_c^r+\widetilde{\mathbf{E}}_c:\boldsymbol{\varepsilon}, & E_v(\boldsymbol{\varepsilon})=E_v^r+\widetilde{\mathbf{E}}_v:\boldsymbol{\varepsilon},\\ N_c(\boldsymbol{\varepsilon})=N_c^r+\widetilde{\mathbf{N}}_c:\boldsymbol{\varepsilon}, & N_v(\boldsymbol{\varepsilon})=N_v^r+\widetilde{\mathbf{N}}_v:\boldsymbol{\varepsilon},\end{cases} \tag{3.6}$$

where the superscript r denotes the value of the parameter in the relaxed state ($\boldsymbol{\varepsilon}=\mathbf{0}$) and where the rank-2 tensors $\widetilde{\mathbf{E}}_c$, $\widetilde{\mathbf{E}}_v$, $\widetilde{\mathbf{N}}_c$ and $\widetilde{\mathbf{N}}_v$ account for first-order strain-induced changes in the corresponding quantities.

Similarly, the mobilities of electrons and holes are expressed as

$$\mathbf{M}_n(\boldsymbol{\varepsilon})=\mathbf{M}_n^r+\widetilde{\mathbf{M}}_n:\boldsymbol{\varepsilon},\qquad \mathbf{M}_p(\boldsymbol{\varepsilon})=\mathbf{M}_p^r+\widetilde{\mathbf{M}}_p:\boldsymbol{\varepsilon}, \tag{3.7}$$

where $\widetilde{\mathbf{M}}_n$ and $\widetilde{\mathbf{M}}_p$ are rank-4 tensors. All the tilde coefficients that account for change per unit strain of the electronic parameters are material properties.

[15] Note that in (3.6) we assume that these electronic parameters depend linearly on the strain directions. This might not always be the case, e.g., the valence band of silicon E_v is not a linear function of the components ε_{ij} (Appendix A). However, the developments that follow still hold at first order in $\boldsymbol{\varepsilon}$.

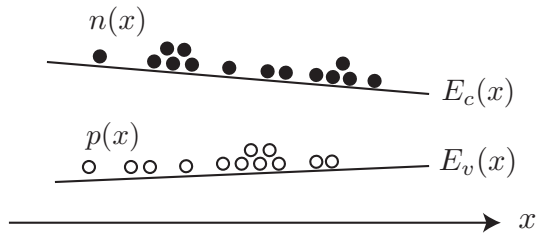

Fig. 4. As a result of nonuniform strains, the band edge energies of the conduction and valence bands, as well as the densities of states and the charge-carrier mobilities depend on position.

The spatial variations of the electronic parameters E_c, E_v, N_c, N_v, $\mathbf{M}_n$ and $\mathbf{M}_p$ are obtained by substituting the strain field (3.2) and (3.5) in (3.6) and (3.7), thus yielding

$$\begin{cases} E_c(x,y,z) = E_c^0 + \kappa \widehat{E}_c(x-x_0), & E_v(x,y,z) = E_v^0 + \kappa \widehat{E}_v(x-x_0), \\ N_c(x,y,z) = N_c^0 + \kappa \widehat{N}_c(x-x_0), & N_v(x,y,z) = N_v^0 + \kappa \widehat{N}_v(x-x_0), \\ m_n(x,y,z) = m_n^0 + \kappa \widehat{m}_n(x-x_0), & m_p(x,y,z) = m_p^0 + \kappa \widehat{m}_p(x-x_0), \end{cases} \tag{3.8}$$

where m_n and m_p are the xx-components of the rank-2 mobility tensors $\mathbf{M}_n$ and $\mathbf{M}_p$. The constants E_c^0, E_v^0, N_c^0, N_v^0, m_n^0, and m_p^0, as well as the coefficients $\widehat{E}_c$, $\widehat{E}_v$, $\widehat{N}_c$, $\widehat{N}_v$, $\widehat{m}_n$, and $\widehat{m}_p$ are calculated in Appendix A for a linearly elastic material with cubic symmetry, subjected to the strain state considered. As a result, electrons and holes evolve in spatially nonuniform conduction and valence bands as illustrated in Fig. 4.

3.1.3. Governing equations of the one-dimensional model

We consider either a polycrystalline material or an orthotropic crystalline material whose x-direction is a principal crystallographic direction. In either case, the mobility tensors $\mathbf{M}_n(\boldsymbol{\varepsilon})$ and $\mathbf{M}_p(\boldsymbol{\varepsilon})$ in the deformed configuration are diagonal when written in the (x, y, z) coordinate system. Hence, by (2.56) and the y- and z-translations invariance, the currents of electrons and holes have no components along these directions, i.e., $\boldsymbol{\jmath}_n = \jmath_n(x)\mathbf{e}_x$ and $\boldsymbol{\jmath}_p = \jmath_p(x)\mathbf{e}_x$. In addition we consider only the steady-state regime, i.e., all variables are independent of time.

Under these assumptions, the electronic transport problem (2.5), (2.12), (2.13) and (2.56) reduces to a one-dimensional system of equations whose unknowns are the fields $\varphi(x)$, $n(x)$, and $p(x)$. With the prime denoting the x-derivative, we obtain

$$\begin{cases} \epsilon_r \varphi'' = q\rho\big(n - p - C(x)\big), \\ \jmath_n' = -R, \qquad \jmath_n = -\dfrac{k\theta\rho}{q} m_n(x) n' + \dfrac{\rho}{q} m_n(x) n\Big[q\varphi' - E_c'(x) + k\theta\big(\ln(N_c(x))\big)'\Big], \\ \jmath_p' = -R, \qquad \jmath_p = -\dfrac{k\theta\rho}{q} m_p(x) p' + \dfrac{\rho}{q} m_p(x) p\Big[-q\varphi' + E_v'(x) + k\theta\big(\ln(N_v(x))\big)'\Big]. \end{cases} \tag{3.9}$$

In $(3.9)_{2,3}$, the recombination–generation R and intrinsic concentration n_i given by (2.57) and (2.58) are written as functions of x:

$$R(x) = \frac{\rho\,(pn - n_i^2(x))}{\tau_p(n + n_i(x)) + \tau_n(p + n_i(x))}, \qquad n_i^2(x) = N_c(x)N_v(x)\exp\left[\frac{-(E_c(x) - E_v(x))}{k\theta}\right]. \tag{3.10}$$

The system of field Eqs. (3.9) and (3.10) is supplemented by the boundary conditions at the ohmic contact $x = 0$ and $x = l$ encapsulated in (2.63):

$$\begin{cases} n - p - C = 0, \\ np = n_i^2, \\ \varphi = \varphi_{bin} + \varphi_{app}. \end{cases} \tag{3.11}$$

The reader can refer to Section 2.3.4 for the physical meaning of these boundary conditions. Recall that (3.11) is the decomposition of the electric potential at each end into the built-in potential φ_{bin} and the externally applied voltage φ_{app}. The difference in the built-in electric potential $\varphi_{bin}(l) - \varphi_{bin}(0)$ corresponds to the voltage drop that exists naturally at equilibrium, i.e., in absence of external voltage bias.

Finally, at the interface $x = x_0$, in the absence of surface charges, the fields n, p and φ are continuous.

3.2. Asymptotic analysis

In this section, we solve the one-dimensional electronic boundary-value problem (3.9)–(3.11) by means of asymptotic analysis.

Table 1
Scaling of the variables for the electronic boundary-value problem.

Scaling factor	Related variable	Physical meaning
l	x	Space variable
$1/l$	κ	Curvature
$k\theta$	E_c, E_v, $\widehat{E}_c$, $\widehat{E}_v$	Band edge energy
$U_T := k\theta/q$	φ, V	Electric potential, voltage
$\overline{C} := \max(N_a, N_d)$	n, p, C, n_i, N_c, N_v, $\widehat{N}_c$, $\widehat{N}_v$	Number of particles per unit mass
$\overline{m} := \max(m_n^r, m_p^r)$	m_n, m_p, $\widehat{m}_n$, $\widehat{m}_p$	Mobility
$\bar{\jmath} := \dfrac{U_T \overline{m} \rho \overline{C}}{l}$	$\jmath_n$, $\jmath_p$	Current of particles
$\bar{\jmath}_e := q\bar{\jmath}$	$\jmath$	Total electric current
$\overline{\tau} := \dfrac{l^2}{U_T \overline{m}}$	τ_n, τ_p	Electron and hole lifetimes
$\overline{R} := \rho\overline{C}/\overline{\tau}$	R	Recombination rate

3.2.1. Non-dimensionalization

We introduce non-dimensional variables (Markowich, 1986) in Table 1. Three small dimensionless parameters are identified for the ensuing asymptotic analysis of the problem. The first parameter, $\lambda := \left(\epsilon_r U_T/q\rho\overline{C}l^2\right)^{1/2}$, is the scaled *Debye length*, which measures the width of the space charge layer that exists at the $p-n$ interface; it is typically of the order of 10^{-5}. The second parameter, $\delta := \left(n_i^0/\overline{C}\right)^{1/2}$, is the dimensionless number that gives the *doping strength* relative to the intrinsic concentration $n_i^0 := \sqrt{N_c^0 N_v^0}\exp[-(E_c^0 - E_v^0)/2k\theta]$ at the interface $x = x_0$. For the problem at hand, this number is of order 10^{-4} to 10^{-3}. Finally, κ is the *dimensionless curvature*, which for the application of interest is of order 10^{-3}.

3.2.2. First-order asymptotics with respect to curvature and doping

We will approximate the Eqs. (3.9), (3.10) and the boundary conditions (3.11) by neglecting all terms that are second order in κ and δ. To alleviate an already cumbersome notation, each dimensionless variable is denoted by the same symbol as its dimensional counterpart. In addition, the prime now corresponds to the derivative with respect to the dimensionless space variable x.

Starting with the spatial variations of the electronic parameters $(3.8)_{3,4}$ we have the following first-order approximation in κ:

$$\left(\ln(N_c(x))\right)' = \frac{\widehat{N}_c}{N_c^0}\kappa + O(\kappa^2), \qquad \left(\ln(N_v(x))\right)' = \frac{\widehat{N}_v}{N_v^0}\kappa + O(\kappa^2). \tag{3.12}$$

Appealing to $(3.8)_{1,2}$ and $(3.10)_2$ in conjunction with the approximation $1+\epsilon = \exp(\epsilon) + O(\epsilon^2)$ for $|\epsilon| < 1$, we approximate $n_i^2(x)$ by

$$\begin{aligned} n_i^2(x) &= N_c^0 N_v^0 \exp\left[-(E_c^0 - E_v^0)\right] \exp\left[-\kappa\left(\widehat{E}_c - \widehat{E}_v - \frac{\widehat{N}_c}{N_c^0} - \frac{\widehat{N}_v}{N_v^0}\right)(x - x_0)\right] + O(\kappa^2) \\ &= \delta^4 \exp\left[-\kappa(\underbrace{\widehat{E}_c^e - \widehat{E}_v^e}_{\widehat{E}_g^e})(x - x_0)\right] + O(\kappa^2), \end{aligned} \tag{3.13}$$

where $\widehat{E}_g^e := \widehat{E}_c^e - \widehat{E}_v^e$ is the *effective band gap coefficient*, and $\widehat{E}_c^e := \widehat{E}_c - \widehat{N}_c/N_c^0$ and $\widehat{E}_v^e := \widehat{E}_v + \widehat{N}_v/N_v^0$ are the *effective band edge coefficients*, which combine the effect of band edge level and effective density of states.

With these approximations, the governing Eq. (3.9) can be recast as

$$\begin{cases} \lambda^2\varphi'' = n - p - C(x), \\ \quad \jmath_n' = -R, \qquad \jmath_n = \left(m_n^0 + \kappa\widehat{m}_n(x - x_0)\right)\left[-n' + n(\varphi' - \kappa\widehat{E}_c^e)\right] + O(\kappa^2), \\ \quad \jmath_p' = -R, \qquad \jmath_p = \left(m_p^0 + \kappa\widehat{m}_p(x - x_0)\right)\left[-p' + p(-\varphi' + \kappa\widehat{E}_v^e)\right] + O(\kappa^2), \end{cases} \tag{3.14}$$

where, in view of (3.10),

$$R(x) = \frac{pn - n_i^2(x)}{\tau_p(n + n_i(x)) + \tau_n(p + n_i(x))}, \qquad n_i^2(x) = \delta^4 \exp\left[-\kappa\widehat{E}_g^e(x - x_0)\right] + O(\kappa^2). \tag{3.15}$$

The boundary conditions $(3.11)_{1,2}$ constitute an algebraic system of two equations for two unknowns $n(0)$ and $p(0)$ when evaluated at $x = 0$, and $n(1)$ and $p(1)$ when evaluated at $x = 1$. We write the solution for n and p up to leading order in κ and δ, and complete these boundary conditions with those pertaining to φ:

$$\begin{cases} n(0) = \frac{\delta^4}{N_a}\exp[\kappa\widehat{E}_g^e x_0] + O(\delta^4\kappa^2) + O(\delta^8), \\ p(0) = N_a + O(\delta^4), \\ \varphi(0) = \varphi_{bin}(0) + \varphi_{app}(0), \end{cases} \qquad \begin{cases} n(1) = N_d + O(\delta^4), \\ p(1) = \frac{\delta^4}{N_d}\exp[-\kappa\widehat{E}_g^e(1 - x_0)] + O(\delta^4\kappa^2) + O(\delta^8), \\ \varphi(1) = \varphi_{bin}(1) + \varphi_{app}(1). \end{cases} \tag{3.16}$$

3.2.3. Built-in potential: the $p-n$ junction in the absence of external voltage

The equilibrium case, in which no external voltage is applied, i.e., $\varphi_{app}(0)=\varphi_{app}(1)=0$, is considered for the sole purpose of deriving the electric potential drop $\varphi_{bin}(1)-\varphi_{bin}(0)$ across the junction, which allows the specification of the values of $\varphi_{bin}(0)$ and $\varphi_{bin}(1)$ in the boundary conditions on φ. Under equilibrium, we have $\jmath_n(x)=\jmath_p(x)=0$ for the entire domain (0, 1), which, by $(3.14)_2$, yields

$$-n'(x)+n(x)\left(\varphi'_{bin}(x)-\kappa\widehat{E}^e_c\right)=0 \tag{3.17}$$

Integrating (3.17) between $x=0$ and $x=1$ yields the electric potential drop across the junction:

$$\varphi_{bin}(1)-\varphi_{bin}(0)=\ln\left(\frac{N_dN_a}{\delta^4}\right)+\kappa\left(\widehat{E}^e_v x_0+\widehat{E}^e_c(1-x_0)\right). \tag{3.18}$$

The reference value of the electric potential being arbitrary, $\varphi_{bin}(0)$ and $\varphi_{bin}(1)$ are only required to satisfy (3.18). We hence set the following boundary conditions:

$$\varphi_{bin}(0)=-\ln\left(\frac{N_a}{\delta^2}\right)-\kappa\widehat{E}^e_v x_0,\qquad \varphi_{bin}(1)=\ln\left(\frac{N_d}{\delta^2}\right)+\kappa\widehat{E}^e_c(1-x_0). \tag{3.19}$$

The full expressions of $n(x)$, $p(x)$, $\varphi_{bin}(x)$ in the absence of external voltage could be derived from the system (3.14), however, they are not needed here.

3.2.4. Current–voltage characteristic $\jmath(\mathrm{V})$: the $p-n$ junction under external voltage

We set for the externally applied potential at the extremities of the $p-n$ junction:

$$\varphi_{app}(0)=0,\qquad \varphi_{app}(1)=-V. \tag{3.20}$$

The computation of $\jmath(V)$ is simplified by replacing the variables n and p with new ones, u and v, defined as

$$u:=\delta^{-2}n\exp\left[-\varphi+\kappa\widehat{E}^e_c(x-x_0)\right],\qquad v:=\delta^{-2}p\exp\left[\varphi-\kappa\widehat{E}^e_v(x-x_0)\right]. \tag{3.21}$$

Next, the governing Eq. (3.14) is rewritten in terms of u and v to leading order in κ and δ:

$$\begin{cases}\lambda^2\varphi''=\delta^2\left(u\exp\left[\varphi-\kappa\widehat{E}^e_c(x-x_0)\right]-v\exp\left[-\varphi+\kappa\widehat{E}^e_v(x-x_0)\right]\right)-C(x),\\ \jmath'_n=-R,\qquad \jmath_n=-\delta^2\left(m^0_n+\kappa\widehat{m}_n(x-x_0)\right)u'\exp\left[\varphi-\kappa\widehat{E}^e_c(x-x_0)\right],\\ \jmath'_p=-R,\qquad \jmath_p=-\delta^2\left(m^0_p+\kappa\widehat{m}_p(x-x_0)\right)v'\exp\left[-\varphi+\kappa\widehat{E}^e_v(x-x_0)\right],\end{cases} \tag{3.22}$$

where, in light of (3.15) and (3.21),

$$\begin{aligned}&R(x)=A/B,\ \text{where}\\ &A:=\delta^2\left(uv-1\right)\exp\left[-\kappa\widehat{E}^e_g(x-x_0)\right],\\ &B:=\tau_p\left(u\exp\left[\varphi-\kappa\widehat{E}^e_c(x-x_0)\right]+\exp\left[-\frac{\kappa}{2}\widehat{E}^e_g(x-x_0)\right]\right)\\ &\qquad+\tau_n\left(v\exp\left[-\varphi+\kappa\widehat{E}^e_v(x-x_0)\right]+\exp\left[-\frac{\kappa}{2}\widehat{E}^e_g(x-x_0)\right]\right).\end{aligned} \tag{3.23}$$

By (3.19)–(3.21), the boundary conditions (3.16) take the form

$$\begin{cases}u(0)=1,\\ v(0)=1,\\ \varphi(0)=-\ln\left(\frac{N_a}{\delta^2}\right)-\kappa\widehat{E}^e_v x_0,\end{cases}\qquad\begin{cases}u(1)=\exp[V],\\ v(1)=\exp[-V],\\ \varphi(1)=\ln\left(\frac{N_d}{\delta^2}\right)+\kappa\widehat{E}^e_c(1-x_0)-V.\end{cases} \tag{3.24}$$

In the system of Eqs. (3.22)–(3.24), the small parameter λ multiplies the highest derivative of φ, which implies the existence of a boundary layer at $x=x_0$, where $C(x)$ is discontinuous. In what follows, we outline the main steps of the matched asymptotic expansion analysis used to solve the singular perturbation problem associated with the small parameters λ and δ and refer the reader to Markowich (1986) for further details. The small parameter κ, which embeds strain effects, introduces a regular perturbation of the case $\kappa=0$. We solve the resulting problem by means of the Poincaré asymptotic expansion.

In the boundary layer, we introduce the fast variable $\widehat{x}$:

$$\widehat{x}=\frac{x-x_0}{\lambda}. \tag{3.25}$$

Away from the boundary layer, we expect u, v and φ to vary on the slow x-scale. We thus introduce the *outer expansions*:

$$\begin{cases}u(x;\lambda,\delta,\kappa)=\overline{u}(x;\delta,\kappa)+O(\lambda),\\ v(x;\lambda,\delta,\kappa)=\overline{v}(x;\delta,\kappa)+O(\lambda),\\ \varphi(x;\lambda,\delta,\kappa)=\overline{\varphi}(x;\delta,\kappa)+O(\lambda).\end{cases} \tag{3.26}$$

In the boundary layer, we write down the *inner expansions*:

$$\begin{cases} u(x;\lambda,\delta,\kappa) = \overline{u}(x;\delta,\kappa) + \widehat{u}(\widehat{x};\delta,\kappa) + O(\lambda), \\ v(x;\lambda,\delta,\kappa) = \overline{v}(x;\delta,\kappa) + \widehat{v}(\widehat{x};\delta,\kappa) + O(\lambda), \\ \varphi(x;\lambda,\delta,\kappa) = \overline{\varphi}(x;\delta,\kappa) + \widehat{\varphi}(\widehat{x};\delta,\kappa) + O(\lambda). \end{cases} \tag{3.27}$$

The matching condition reads

$$\lim_{\widehat{x}\to\pm\infty} [\widehat{u},\widehat{v},\widehat{\varphi}](\widehat{x};\delta,\kappa) = [0,0,0]. \tag{3.28}$$

In the case $\kappa = 0$, Markowich (1986) shows that $\widehat{u}$ and $\widehat{v}$ are identically zero for all $\widehat{x}\in\mathbb{R}$ and establishes the continuity of $\overline{u}$ and $\overline{v}$ at $x = x_0$. It can be shown that these results hold true in the case $\kappa \neq 0$.

We now consider the outer problem for $\kappa \neq 0$. Inserting the outer expansions (3.26) in the system (3.22) and equating the zeroth-order terms in λ, $(3.22)_1$ yields

$$0 = \delta^2\left(\overline{u}\exp\left[\overline{\varphi} - \kappa\widehat{E}_c^e(x-x_0)\right] - \overline{v}\exp\left[-\overline{\varphi} + \kappa\widehat{E}_v^e(x-x_0)\right]\right) - C(x). \tag{3.29}$$

The remaining equations, $(3.22)_{2,3}$–(3.24) are unchanged but apply now to the overlined variables (i.e., to the outer expansions).

The solution of the outer problem on the intervals $(0, x_0)$ and $(x_0, 1)$ is detailed in Appendix B. To find the $j(V)$ relation, we need the currents $j_n(x)$ and $j_p(x)$, which are computed on $(0, x_0)$ and $(x_0, 1)$, respectively, and are evaluated at $x = x_0$:

$$\begin{cases} j_n(x_0) = -\dfrac{\delta^4 m_n^0\left(\exp[V]-1\right)}{N_a L_n^0}\left[\coth\left(\dfrac{x_0}{L_n^0}\right) + \kappa\left(\dfrac{\widehat{E}_g^e L_n^0}{2} - \dfrac{\widehat{m}_n}{4m_n^0}\left(L_n^0 + \dfrac{x_0^2}{L_n^0\sinh^2\left(\dfrac{x_0}{L_n^0}\right)}\right)\right)\right], \\ j_p(x_0) = \dfrac{\delta^4 m_p^0\left(\exp[V]-1\right)}{N_d L_p^0}\left[\coth\left(\dfrac{1-x_0}{L_p^0}\right) - \kappa\left(\dfrac{\widehat{E}_g^e L_p^0}{2} - \dfrac{\widehat{m}_p}{4m_p^0}\left(L_p^0 + \dfrac{(1-x_0)^2}{L_p^0\sinh^2\left(\dfrac{1-x_0}{L_p^0}\right)}\right)\right)\right], \end{cases} \tag{3.30}$$

where the diffusion lengths of electrons and holes are given by $L_n^0 := \sqrt{\tau_n m_n^0}$ and $L_p^0 := \sqrt{\tau_p m_p^0}$. Subtracting $(3.22)_2$ from $(3.22)_3$ and integrating over x, we establish that the total electric current

$$j(x) := j_p(x) - j_n(x) \tag{3.31}$$

is uniform on $(0, 1)$. We denote it with the constant j and evaluate (3.31) at $x = x_0$ which is the only point where both j_n and j_p are known. We therefore have

$$j = \left(\exp[V]-1\right) j_{sat}, \tag{3.32}$$

where the saturation current j_{sat} is given by

$$\begin{aligned} j_{sat} = {} & \frac{\delta^4 m_n^0}{N_a L_n^0}\coth\left(\frac{x_0}{L_n^0}\right) + \frac{\delta^4 m_p^0}{N_d L_p^0}\coth\left(\frac{1-x_0}{L_p^0}\right) \\ & + \kappa\left\{\frac{\delta^4 m_n^0}{N_a}\left[\frac{\widehat{E}_g^e}{2} - \frac{\widehat{m}_n}{4m_n^0}\left(1 + \frac{x_0^2}{(L_n^0)^2\sinh^2\left(\frac{x_0}{L_n^0}\right)}\right)\right] - \frac{\delta^4 m_p^0}{N_d}\left[\frac{\widehat{E}_g^e}{2} - \frac{\widehat{m}_p}{4m_p^0}\left(1 + \frac{(1-x_0)^2}{(L_p^0)^2\sinh^2\left(\frac{1-x_0}{L_p^0}\right)}\right)\right]\right\}. \end{aligned} \tag{3.33}$$

The above Eqs. (3.32) and (3.33) give the $j(V)$ characteristic for a strained $p-n$ junction. Note that, at zeroth-order in κ, (3.33) reduces to the Shockley equation of a rigid $p-n$ junction (see e.g., Markowich et al., 1990, Section 4.2).

Fig. 5 shows the solution on the outer domain of the original dimensionless problem (3.14)–(3.16), in terms of the carrier concentrations n and p, and the currents j_n, j_p and j of electrons, holes and electric current, respectively. Note the presence of a boundary layer at the $p-n$ interface $x = x_0$ for the carrier concentrations whereas the currents remain continuous. Finally, we rewrite j_{sat} in terms of dimensional variables:

$$\begin{aligned} \frac{J_{sat}}{qU_T(\rho n_i^0)^2} = {} & \frac{m_n^0}{(\rho N_a)L_n^0}\coth\left(\frac{x_0}{L_n^0}\right) + \frac{m_p^0}{(\rho N_d)L_p^0}\coth\left(\frac{l-x_0}{L_p^0}\right) \\ & + \kappa\left\{\frac{m_n^0}{\rho N_a}\left[\frac{\widehat{E}_g^e}{2kT} - \frac{\widehat{m}_n}{4m_n^0}\left(1 + \frac{x_0^2}{(L_n^0)^2\sinh^2\left(\frac{x_0}{L_n^0}\right)}\right)\right] - \frac{m_p^0}{\rho N_d}\left[\frac{\widehat{E}_g^e}{2kT} - \frac{\widehat{m}_p}{4m_p^0}\left(1 + \frac{(l-x_0)^2}{(L_p^0)^2\sinh^2\left(\frac{l-x_0}{L_p^0}\right)}\right)\right]\right\}, \end{aligned} \tag{3.34}$$

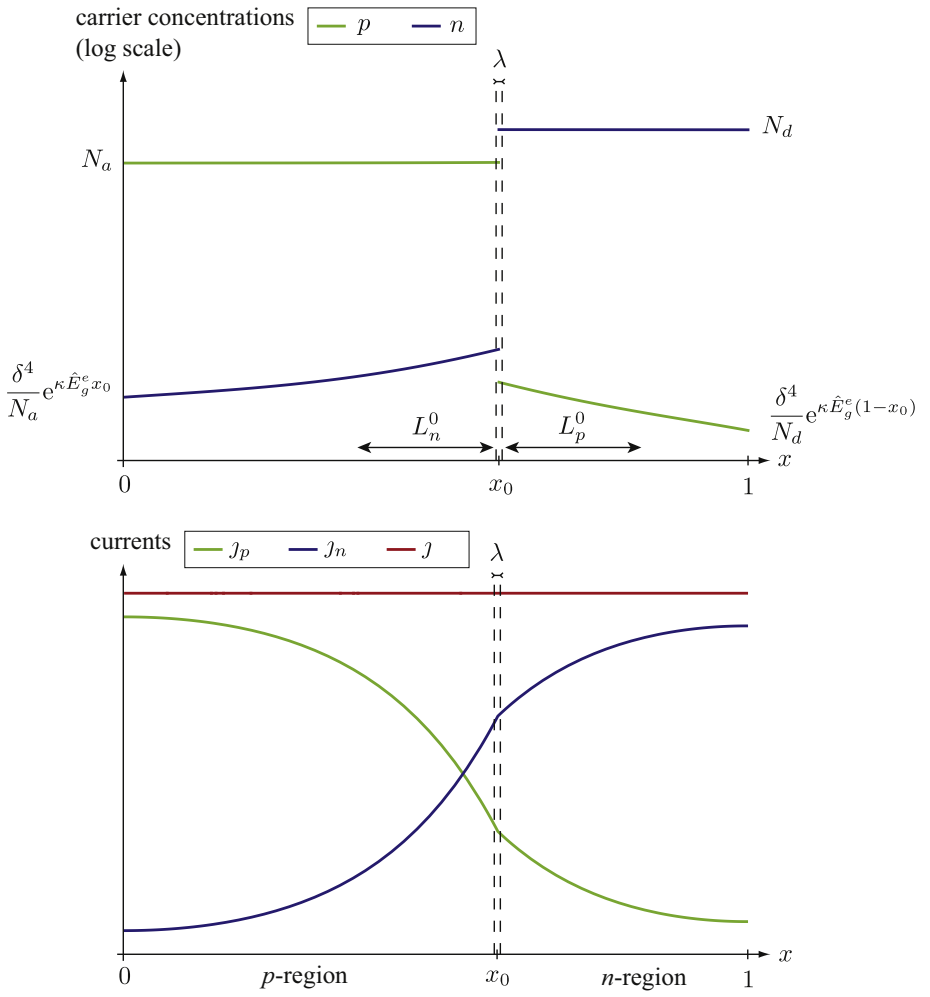

Fig. 5. Electron and hole densities and currents in the $p-n$ junction, solution of the problem (3.14)–(3.16) on the outer domain $(0, x_0)\cup(x_0, 1)$. The explicit forms of the functions n and p are obtained from the relation (3.22) combined with (B.2), (B.5), (B.7), (B.9), (B.11), (B.14), (B.15) and (B.18). The expressions of the current $\jmath_n$, $\jmath_p$ and $\jmath$ can also be made explicit by combining the same set of equations with (B.4) and (3.31).

with the dimensional diffusion lengths defined as $L_n^0 := \sqrt{U_T \tau_n m_n^0}$ and $L_p^0 := \sqrt{U_T \tau_p m_p^0}$.

We can understand the different physical processes underlying the macroscopic strain-induced changes in current by considering each strain-related coefficient in (3.34). The effect of the strain-dependent mobilities appears in the coefficients m_n^0, m_p^0, L_n^0, L_p^0, $\widehat{m}_n$ and $\widehat{m}_p$, whereas n_i^0 and $\widehat{E}_g^e$ account for the strain dependence of band energy levels and densities of states together. Depending on the material and the directions of strain, these microscopic effects can either sum up or compensate each other, resulting in a small or large strain effect on the current. For each one of these effects we can distinguish in (3.34) between the change in current that exists if the junction is uniformly strained with strain $\boldsymbol{\varepsilon}^0$ (accounted for by parameters with superscript 0) and the change due to bending with curvature κ.

3.3. Monocrystalline silicon solar cell

We now consider a typical monocrystalline silicon solar cell subjected to bending and apply the results of Section 3.2 to investigate the effect of strain on its characteristic $\jmath(V)$. The current $\jmath(V)$ given by (3.32) corresponds to what is called in photovoltaics, the *dark current* of the solar cell. It is the current that circulates through the cell under external voltage V and in the absence of illumination. We show in Section 3.3.1 how the change in dark current can be computed from the asymptotic solution of Section 3.2 and, in Section 3.3.2, we calculate and discuss this strain-effect for some typical strain states.

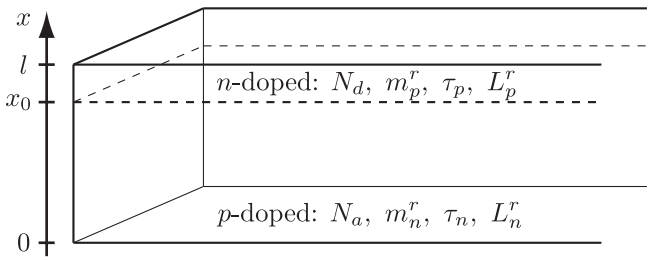

Fig. 6. Typical crystalline silicon solar cell geometry with a thin n-doped emmiter and a thick p-doped base.

Table 2
Typical properties of the monocrystalline silicon solar cell (see Nelson, 2003).

Property	Base p-Si	Emmiter n^+-Si
Width (μm)	$x_0 = 300$	$l - x_0 = 0.5$
Doping (cm^{-3})	$N_a = 1 \times 10^{16}$	$N_d = 1 \times 10^{19}$
Mobility (cm^2 V^{-1} s^{-1})	$m_n^r = 1544$	$m_p^r = 77$
Carrier lifetime (s)	$\tau_n = 5 \times 10^{-6}$	$\tau_p = 1 \times 10^{-6}$
Diffusion length (μm)	$L_n^r = 140$	$L_p^r = 14$

3.3.1. Strain-induced changes of the dark current

Consider the diamond lattice structure of silicon, assume that the principal crystallographic directions ⟨100⟩ are aligned with the (x, y, z) directions (Fig. 6). The cell consists of a pn^+-junction (i.e., asymmetrically doped: $N_d \gg N_a$) whose characteristics are given in Table 2. Note that the thickness of the n^+-region (the *emitter*) is about one thousand times smaller than the thickness of the p-doped region (the *base*), the junction interface is thus effectively located at the boundary plane $x = l$.

As an application of the previous theory, we aim at computing the change in dark current when the cell is under bending about the z-direction. Notice that Eq. (3.32) has been derived under the assumption of Dirichlet boundary conditions (3.16) expressing that the densities of electrons and holes at the boundaries $x = 0$ and $x = l$ are the corresponding equilibrium densities. In practice, at the boundaries of a solar cell there is an inevitable surface recombination proportional to the deviation of the densities from their equilibrium values. For reasons to be explained below, the surface recombination can be neglected in the problem considered.

Starting with the dimensional version of (3.31), we evaluate the current at $x = x_0$,

$$J = q\big(J_p(x_0) - J_n(x_0)\big). \tag{3.35}$$

From (3.30), we conclude that the doping strength asymmetry between the regions n^+ and p ($N_d \gg N_a$), results in a current $J_p(x_0)$ (associated to diffusion of holes in the emitter n^+) which is at least two orders of magnitude smaller than the current $J_n(x_0)$ (associated to diffusion of electrons in the base p), i.e., $J_p(x_0) \ll J_n(x_0)$. This holds even in presence of surface recombination. Further, since $L_n^0 \ll x_0$, surface recombination for $J_n(x_0)$ can be safely ignored, given that it only affects the negligible hole-diffusion current $J_p(x_0)$. It follows from (3.34) that the saturation current of the junction reduces to the contribution of $J_n(x_0)$. Since $L_n^0/x_0 \ll 1$, we obtain the simplified expression:

$$J_{sat} = qU_T(\rho n_i^0)^2\left[\frac{m_n^0}{(\rho N_a)L_n^0} + \kappa\left\{\frac{m_n^0}{(\rho N_a)}\left(\frac{\widehat{E}_g^e}{2kT} - \frac{\widehat{m}_n}{4m_n^0}\right)\right\}\right] + O\left(\exp\left[\frac{-2x_0}{L_n^0}\right]\right). \tag{3.36}$$

We now define the relative strain-induced change in dark current Δ_J, where we also linearize the contribution due to $\boldsymbol{\varepsilon}^0$. As a result, we only keep first-order perturbations in κ and in the amplitude of $\boldsymbol{\varepsilon}^0$ (represented by the yy-component ε_{yy}^0), in which case (3.36) yields

$$\Delta_J := \frac{J_{sat}(\varepsilon_{yy}^0, \kappa) - J_{sat}^r}{J_{sat}^r} = \left(\frac{\widehat{m}_n}{2m_n^r} - \frac{\widehat{E}_g^e}{kT}\right)\left(\varepsilon_{yy}^0 - \frac{\kappa L_n^r}{2}\right), \tag{3.37}$$

where $\widehat{E}_g^e$, defined in (3.13), is approximated by:

$$\widehat{E}_g^e = \widehat{E}_c - \widehat{E}_v - kT\left(\frac{\widehat{N}_c}{N_c^r} + \frac{\widehat{N}_v}{N_v^r}\right). \tag{3.38}$$

3.3.2. Results for typical strain states and discussion

Six different cases of strained solar cells are considered as depicted in Fig. 7. The values of the applied strain and the curvature are summarized in Table 3 and have been chosen such that the highest strain in the cell remains lower than 0.2% in compression and in tension, i.e., the typical strains that silicon can sustain without failing.

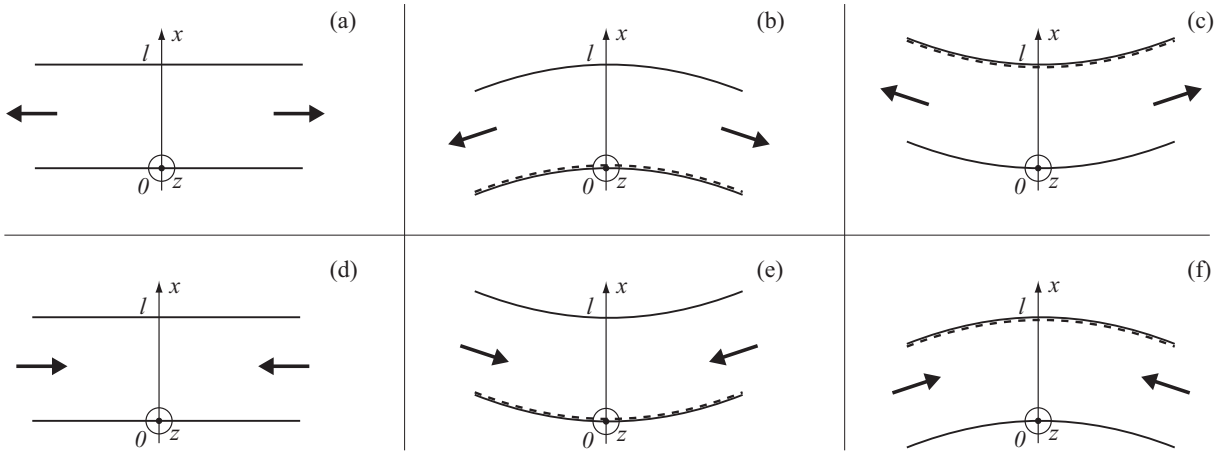

Fig. 7. Six strain states of the solar cell. Cases (a) and (b) correspond to homogeneous strain states, while cases (b), (c), (e) and (f) correspond to nonuniform strain states due to the bending about the z-axis. Cases (a)–(c) correspond to tensile states, whereas cases (d)–(f), are compressive states. The dashed line indicates the neutral plane where $\boldsymbol{\varepsilon} = \mathbf{0}$.

Table 3
Applied radius of curvature $\mathcal{R} = 1/\kappa$ and yy-component of the strain at the interface $x = x_0$ for the strain states depicted in Fig. 7. The cell, described in Table 2, has a thickness $l = 0.3$ mm.

Case	(a)	(b)	(c)	(d)	(e)	(f)
$\mathcal{R} = 1/\kappa$ (mm)	∞	150	−150	∞	−150	150
ε^0_{yy} ($\times 10^{-3}$)	2.0	2.0	0	−2.0	−2.0	0

Table 4
Strain-induced changes in dark current for the six strain states depicted in Fig. 7.

Case	(a)	(b)	(c)	(d)	(e)	(f)
Δ_J (%)	−19	−14	−4	24	19	6

The coefficients entering the yy-component of the strain are given in Table 3, while the remaining strain components are deduced, in the same way as in Section 3.1.1, using the linear constitutive law of silicon in (3.4):

$$\varepsilon_{yy}(x) = \varepsilon^0_{yy} + \kappa x, \quad \varepsilon_{zz}(x) = 0, \quad \varepsilon_{xx}(x) = -\frac{c_{xxyy}}{c_{xxxx}}\varepsilon_{yy}(x), \tag{3.39}$$

where $c_{xxxx} = 166$ GPa and $c_{xxyy} = 64$ GPa (Wortman and Evans, 1965). Since the principal axes of the cubic-symmetry crystal are assumed to be the coordinate axes, the off-diagonal components of $\boldsymbol{\varepsilon}$ vanish.

Using the strain state (3.39), the x-dependence of the six electronic parameters E_c, E_v, N_c, N_v, m_n, m_p in silicon is derived in the Appendix A. We obtain $\widehat{m}_n/2m^r_n = -48$. Further, given the tension-compression asymmetry for the strain dependence of the valence band edge energy and effective density of states (see Eqs. (A.9) and (A.10)) we have for the effective band gap: $\widehat{E}^e_g/kT = 46$ for tension ($\varepsilon_{yy} \geq 0$) and 73 for compression ($\varepsilon_{yy} < 0$).

The strain-induced changes in dark current Δ_J are summarized in Table 4 for the six strain states considered. They show a decrease (resp. increase) in dark current in tension (resp. compression) that can reach 24%.

By comparing values of $\widehat{m}_n/2m^r_n$ and $\widehat{E}^e_g/kT$, we observe that the strain-induced change due to mobility is of the same order as the one due to the energy gap and effective density of states (both included in $\widehat{E}^e_g$). As expected the largest changes correspond to a uniform straining of the cell. The presence of bending is equivalent to a uniform strain change, with the strain at midpoint $x = x_0 - L^r_n/2$ as can be seen from (3.37). Hence, the strain influence is maximal when the strain at the midpoint is maximized.

4. Conclusions

In summary, we have derived a theory for the effect of strain on semiconductors in a manner consistent with the laws of thermodynamics, and applied the resulting model to the study of a $p-n$ junction device under bending.

In the first part, the interactions between mechanics, electrostatics, and electronics are accounted for in a fully coupled continuum model of deformable semiconductors under finite strain. We find that, for the specific case of crystalline semi-

conductors, the dominant effect is the influence of strain on the electronic transport properties. Further, in this case, electrostatic and electronic contributions to the total stress are negligible. As a result, the mechanical equilibrium can be solved separately to compute the strain field, which subsequently enters the electronic problem through the strain-dependent electronic parameters (i.e., the band edge energies, the densities of states, and the mobilities). Nonetheless, the fully coupled formulation shows the existence of an electronic contribution to the stress which, to the best of our knowledge, has not been mentioned in the literature. Notwithstanding the small magnitude of this electronic-induced stress for non-degenerate crystalline semiconductors, it is an order of magnitude larger than the electrostatic (Maxwell) stress.

In the second part, we apply the general theory to determine the effect of bending on the current–voltage characteristic of a $p-n$ junction. To this end, we solve the generalized drift–diffusion equations in a inhomogeneous linear strain field. This provides, at first order in the applied curvature, the change induced in the current. While it is well known in the literature that the inhomogeneous character of a semiconductor requires the use of the generalized form of the drift–diffusion equations, they are rarely solved in practical device problems. By computing the characteristic of a $p-n$ junction subjected to bending, strain non-uniformities are systematically accounted for in a drift–diffusion framework for the first time. We apply our result to the case of a monocrystalline silicon solar cell subjected to bending and find that changes in dark current are up to 20% for strains of 0.2%. Finally, by comparing various uniform and nonuniform strain fields, we find that the largest dark current changes are expected for the uniform strain loadings.

In view of the importance of strained silicon technology in various electronic applications, e.g., in strained MOSFETs (Chu et al., 2009) and in flexible electronics (Xu et al., 2015), the thermodynamically consistent formulation of the electronic problem in the presence of non-uniform strain fields presented here has potential use in other settings. While for the $p-n$ junction problem under consideration analytical asymptotic methods are sufficient to determine the first-order curvature effect, the computation of strain effects for more complex geometries and strain fields requires a numerical approach.

Acknowledgments

This work is supported by the “IDI2015” project funded by the IDEX Paris-Saclay, ANR-11-IDEX-0003-02. Helpful discussions with Prof. Pere Roca i Cabarrocas are gratefully acknowledged. We would also like to thank the reviewers for their constructive comments that lead us to improve an earlier version of this paper.

Appendix A. Choice of the strain-dependent electronic parameters

The first part of this appendix pertains to the derivation of the strain-dependent coefficients for the 1D boundary value problem in Section 3.1.3. The second part gives their numerical values for the $p-n$ junction in the monocrystalline silicon solar cell application considered in Section 3.3.

A1. 3D-to-1D reduction of the strain-dependent electronic parameters

Using the strain field $\boldsymbol{\varepsilon}(x)$ in (3.2) and (3.5) into the three-dimensional version of the strain-dependent electronic parameters (3.6) and (3.7), we obtain for the conduction and valence band edges:

$$E_c(x) = E_c^0 + \kappa \widehat{E}_c (x - x_0), \qquad E_v(x) = E_v^0 + \kappa \widehat{E}_v (x - x_0), \tag{A.1}$$

with

$$\begin{cases} E_c^0 := E_c^r - \dfrac{c_{xxyy}}{c_{xxxx}} \widetilde{E}_{c,xx} (\varepsilon_{yy}^0 + \varepsilon_{zz}^0) + \widetilde{E}_{c,yy} \varepsilon_{yy}^0 + \widetilde{E}_{c,zz} \varepsilon_{zz}^0, \\ \widehat{E}_c := -\dfrac{c_{xxyy}}{c_{xxxx}} \widetilde{E}_{c,xx} (\alpha_y + \alpha_z) + \widetilde{E}_{c,yy} \alpha_y + \widetilde{E}_{c,zz} \alpha_z. \end{cases} \tag{A.2}$$

Here, c_{xxxx} and c_{xxyy} are the normal and transverse components of the elasticity tensor $\mathbf{c}$ and $\widetilde{E}_{c,xx}$, $\widetilde{E}_{c,yy}$, and $\widetilde{E}_{c,zz}$ denote the Cartesian components of the tensor $\widetilde{\mathbf{E}}_c$. For the conduction band edge, E_v^0 and $\widehat{E}_v$ follow relations strictly analogous to (A.2).

We have similar relations for the effective densities of states:

$$N_c(x) = N_c^0 + \kappa \widehat{N}_c (x - x_0), \qquad N_v(x) = N_v^0 + \kappa \widehat{N}_v (x - x_0), \tag{A.3}$$

with N_c^0, N_v^0, $\widehat{N}_c$, $\widehat{N}_v$ defined in strict analogy with (A.2).

For the mobilities, due to the assumed constitutive and loading symmetries, we need the xx-component of the mobility tensors $\mathbf{M}_n$ and $\mathbf{M}_p$ denoted by

$$m_n := M_{n,xx}, \qquad m_p := M_{p,xx}. \tag{A.4}$$

Inserting (3.2) and (3.5) in (3.7) we obtain:

$$m_n(x) = m_n^0 + \kappa \widehat{m}_n (x - x_0), \qquad m_p(x) = m_p^0 + \kappa \widehat{m}_p (x - x_0), \tag{A.5}$$

where

$$\begin{cases} m_n^0 := M_{n,xx}^r - \dfrac{c_{xxyy}}{c_{xxxx}}\widetilde{M}_{n,xxxx}(\varepsilon_{yy}^0 + \varepsilon_{zz}^0) + \widetilde{M}_{n,xxyy}\varepsilon_{yy}^0 + \widetilde{M}_{n,xxzz}\varepsilon_{zz}^0, \\ \widehat{m}_n := -\dfrac{c_{xxyy}}{c_{xxxx}}\widetilde{M}_{n,xxxx}(\alpha_y + \alpha_z) + \widetilde{M}_{n,xxyy}\alpha_y + \widetilde{M}_{n,xxzz}\alpha_z, \end{cases} \tag{A.6}$$

and analogous relations for m_p^0 and $\widehat{m}_p$.

A2. Strain-dependence of the electronic properties of silicon

Next, we select on the basis of the physics literature pertaining to the effect of strain on the electronic properties of silicon the numerical values for the aforementioned electronic parameters needed for the application in Section 3.3.

Although the influence of strain on the electronic properties of monocrystalline silicon has been studied over more than fifty years, it is still an open subject and one can find in the literature constants that vary by more than 30% as seen in Van de Walle (1989), Friedel et al. (1989), Fischetti and Laux (1996). While in the solid-state physics literature the effect of strain refers to the sub-bands composing the conduction and valence bands, we introduce here, through linearizations, a two-band equivalent description of the conduction and valence bands that combines the effect of strain on their constitutive sub-bands.

Consider first the band edges $E_c(\boldsymbol{\varepsilon})$ and $E_v(\varepsilon)$ and the effective densities of state (DOS) $N_c(\boldsymbol{\varepsilon})$, $N_v(\varepsilon)$ whose computations are based on the so-called deformation potentials that have been introduced by Bardeen and Shockley (1950) (see e.g., Bir et al., 1974; Fischetti and Laux, 1996; Friedel et al., 1989; Herring and Vogt, 1956; Van de Walle, 1989 and a synthesis in Creemer, 2002, Section 2.2.2).

A3. Conduction band edge energy

The shift of the band edge of the conduction band depends on the strain-induced volume change through (Herring and Vogt, 1956):

$$\Delta E_c(\boldsymbol{\varepsilon}) := E_c(\boldsymbol{\varepsilon}) - E_c^r = \left(\Xi_d + \frac{1}{3}\Xi_u\right)\mathrm{Tr}(\boldsymbol{\varepsilon}). \tag{A.7}$$

In view of the strain triaxiality (3.39) of the problem considered, it reads as a function of x:

$$\Delta E_c(x) = \widehat{E}_c\varepsilon_{yy}(x), \qquad \widehat{E}_c = \left(1 - \frac{c_{xxyy}}{c_{xxxx}}\right)\left(\Xi_d + \frac{1}{3}\Xi_u\right). \tag{A.8}$$

For numerical application, we take the values of Fischetti and Laux (1996): $\Xi_d = 1.1\,\mathrm{eV}$ and $\Xi_u = 10.5\,\mathrm{eV}$ that give $\widehat{E}_c = 2.83\,\mathrm{eV}$.

A4. Valence band edge energy

The strain effect on the valence band edge $E_v(\varepsilon)$ and DOS $N_v(\varepsilon)$ is more complicated and less well understood than for the conduction band. Due to the complex structure of the valence band, the band edge shift, although linear with respect to the strain amplitude, is not linear with respect to the directions of the strain (Kanda, 1967). In addition, the strain effect depends on the sign of the strain components which implies, regarding silicon, that the validity of (3.36) is restricted to situations where the strain keep the same sign in the whole $p-n$ junction. In view of the stress triaxiality (3.39), we compute $\Delta E_v(x)$:

$$\Delta E_v(x) = E_v(x) - E_v^r = \begin{cases} \widehat{E}_v^+\varepsilon_{yy}(x) & \text{for } \varepsilon_{yy}(x) \geq 0, \\ \widehat{E}_v^-\varepsilon_{yy}(x) & \text{for } \varepsilon_{yy}(x) < 0, \end{cases} \tag{A.9}$$

with $\widehat{E}_v^+ = 3.26\,\mathrm{eV}$ and $\widehat{E}_v^- = -0.68\,\mathrm{eV}$ obtained from the values of deformation potentials of Fischetti and Laux (1996).

A5. Effective densities of state

The DOS N_c of the conduction band is little affected by strain compared to the other parameters so that it can be assumed constant (Creemer and French, 2000; Kanda, 1967). Hence, $\widehat{N}_c = 0$. For the valence band the change in DOS $\Delta N_v(\varepsilon)$ has been the object of fewer studies. However, Creemer (2002) recently pointed that this effect is of the same order as the bands edge shift. For simplicity, we assume a linear dependence of $\Delta N_v(\varepsilon)$ with respect to $\boldsymbol{\varepsilon}$ of the type of $(3.6)_2$ and appeal to the computation of Creemer to derive $\widetilde{\mathbf{N}}_v$. Taking into account the stress triaxiality of the problem considered, this leads to spatial variation of N_v of the form

$$\Delta N_v(x) = N_v(x) - N_v^r = \begin{cases} \widehat{N}_v^+\varepsilon_{yy}(x) & \text{for } \varepsilon_{yy}(x) \geq 0, \\ \widehat{N}_v^-\varepsilon_{yy}(x) & \text{for } \varepsilon_{yy}(x) < 0, \end{cases} \tag{A.10}$$

where $\widehat{N}_v^+ = -63N_v^r$ and $\widehat{N}_v^- = 63N_v^r$.

A6. Mobilities

Consider now the strain-induced changes in electron and hole mobilities in silicon. These are at the origin of the piezoresistive effect and have been extensively studied both experimentally and theoretically. A comparison of the data of the literature can be found in Table 2.4 of Creemer (2002). It shows a scattering of about 20%. In light of the strain triaxiality of the problem, the spatial dependence of the *xx*-component of the mobilities reads

$$\Delta m_n(x) = m_n(x) - m_n^r = \widehat{m}_n \varepsilon_{yy}(x), \qquad \Delta m_p(x) = m_p(x) - m_p^r = \widehat{m}_p \varepsilon_{yy}(x). \tag{A.11}$$

Using the experimental values of Smith (1954), we have $\widehat{m}_n = -96 m_n^r$ and $\widehat{m}_p = 2 m_p^r$.

Appendix B. Matched asymptotics: outer problem

In this appendix we solve, on the domains $(0, x_0)$ and $(x_0, 1)$, for the fields $\overline{u}$, $\overline{v}$ and $\overline{\varphi}$ defined in (3.26), the outer problem $(3.22)_{2,3}$, (3.23) and (3.29) along with boundary conditions (3.24).

Solving (3.29) for $\overline{\varphi}$, we obtain

$$\overline{\varphi} = \ln\left(\frac{C + \sqrt{C^2 + 4\delta^4 \overline{u}\overline{v} \exp\left[-\kappa \widehat{E}_g^e (x - x_0)\right]}}{2\delta^2 \overline{u} \exp\left[-\kappa \widehat{E}_c^e (x - x_0)\right]}\right). \tag{B.1}$$

For later use, on appeal to (B.1), we obtain the following approximations:

$$\begin{aligned}
\exp\left[\overline{\varphi} - \kappa \widehat{E}_c^e (x - x_0)\right] &= \begin{cases} \dfrac{\delta^2 \overline{v}}{N_a} \exp\left[-\kappa \widehat{E}_g^e (x - x_0)\right] + O(\delta^6) & \text{for } 0 \le x \le x_0, \\ \dfrac{N_d}{\delta^2 \overline{u}} + O(\delta^2) & \text{for } x_0 \le x \le 1, \end{cases} \\
\exp\left[-\overline{\varphi} + \kappa \widehat{E}_v^e (x - x_0)\right] &= \begin{cases} \dfrac{N_a}{\delta^2 \overline{v}} + O(\delta^2) & \text{for } 0 \le x \le x_0, \\ \dfrac{\delta^2 \overline{u}}{N_d} \exp\left[-\kappa \widehat{E}_g^e (x - x_0)\right] + O(\delta^6) & \text{for } x_0 \le x \le 1. \end{cases}
\end{aligned} \tag{B.2}$$

Inserting (B.1) and $(3.15)_2$ in (3.23), we also have an approximation for the recombination–generation rate R:

$$R = \begin{cases} \dfrac{\delta^4}{\tau_n N_a} (u v - 1) \exp\left[-\kappa \widehat{E}_g^e (x - x_0)\right] + O(\delta^6) & \text{for } 0 \le x \le x_0, \\ \dfrac{\delta^4}{\tau_p N_d} (u v - 1) \exp\left[-\kappa \widehat{E}_g^e (x - x_0)\right] + O(\delta^6) & \text{for } x_0 \le x \le 1. \end{cases} \tag{B.3}$$

Using (B.2), we rewrite $(3.22)_{2,4}$ for the currents of electrons and holes at leading order in δ:

$$\begin{aligned}
\bar{j}_n &= \begin{cases} -\left(m_n^0 + \kappa \widehat{m}_n (x - x_0)\right) \dfrac{\delta^4 \overline{v}\overline{u}'}{N_a} \exp\left[-\kappa \widehat{E}_g^e (x - x_0)\right] & \text{for } 0 \le x \le x_0, \\ -\left(m_n^0 + \kappa \widehat{m}_n (x - x_0)\right) \dfrac{N_d \overline{u}'}{\overline{u}} & \text{for } x_0 \le x \le 1, \end{cases} \\
\bar{j}_p &= \begin{cases} -\left(m_p^0 + \kappa \widehat{m}_p (x - x_0)\right) \dfrac{N_a \overline{v}'}{\overline{v}} & \text{for } 0 \le x \le x_0, \\ -\left(m_p^0 + \kappa \widehat{m}_p (x - x_0)\right) \dfrac{\delta^4 \overline{u}\overline{v}'}{N_d} \exp\left[-\kappa \widehat{E}_g^e (x - x_0)\right] & \text{for } x_0 \le x \le 1. \end{cases}
\end{aligned} \tag{B.4}$$

Although not justified *a priori*, we make ours the assumption of Markowich that u and v are well scaled (i.e., that $\overline{u}, \overline{v}, \overline{u}'$ and $\overline{v}'$ are $O(1)$) to show that $\bar{j}_n$ and $\bar{j}_p$ are $O(\delta^4)$ on $(0, 1)$. Consider first $\bar{j}_n$. By $(B.4)_1$, $\bar{j}_n$ is $O(\delta^4)$ on $(0, x_0)$. Appealing to the continuity of $\bar{j}_n$ across the junction and noticing that $\bar{j}_n$ satisfies on $(x_0, 1)$ Eq. $(3.22)_2$ with R of order $O(\delta^4)$ (see (B.3)), it follows that $\bar{j}_n$ is $O(\delta^4)$ on $(0, 1)$. Through a similar reasoning we also derive that $\bar{j}_p$ is $O(\delta^4)$ on $(0, 1)$.

In view of the expression $(B.4)_1$ for $\bar{j}_n$ on $(x_0, 1)$ and the fact that $\bar{j}_n$ is $O(\delta^4)$, it follows that $\overline{u}'$ is $O(\delta^4)$ on $(x_0, 1)$. By integration over $(x_0, 1)$ we obtain that $\overline{u}$ is constant up to a term of $O(\delta^4)$ on $(x_0, 1)$. Likewise, $\overline{v}$ is constant up to a term of $O(\delta^4)$ on $(0, x_0)$. Therefore, using the boundary conditions $(3.24)_{2,3}$ we have up to terms of $O(\delta^4)$:

$$\begin{cases} \overline{u}(x) = \overline{u}(1) = \exp[V] & \text{for } x \in (x_0, 1), \\ \overline{v}(x) = \overline{v}(0) = 1 & \text{for } x \in (0, x_0). \end{cases} \tag{B.5}$$

Recall that the variable u is associated to n and the variable v is associated to p. Physically, the fact that $\overline{u}$ and $\overline{v}$ are constant at leading order in δ in the regions $(x_0, 1)$ and $(0, x_0)$, respectively, should be related to the fact that $(x_0, 1)$ is

the region where electrons are majority carrier and $(0, x_0)$ is the region where holes are majority carriers. The regions of majority carriers are regions were the concentrations of electrons and holes are governed by the dopant concentration at leading order. At this point, we still need the expressions of the fields $\overline{u}$ and $\overline{v}$ in the domain were electrons and holes are minority carriers respectively.

Combining $(3.22)_2$, (B.3) and $(B.4)_1$, we obtain that $\overline{u}$ is, on $(0, x_0)$, solution of the differential equation

$$\left(m_n^0 + \kappa \widehat{m}_n (x - x_0)\right)\left(\overline{u}'' - \kappa \widehat{E}_g^e \overline{u}'\right) + \kappa \widehat{m}_n \overline{u}' = \frac{\overline{u}' - 1}{\tau_n}. \tag{B.6}$$

Introducing the diffusion length of electrons $L_n^0 := \sqrt{\tau_n m_n^0}$ and defining the variable

$$y := \overline{u} - 1, \tag{B.7}$$

we rewrite (B.6) as an equation for y on $(0, x_0)$,

$$y'' - \frac{1}{(L_n^0)^2} y + \kappa \left(\frac{\widehat{m}_n}{m_n^0} (x - x_0) y'' + \left(\frac{\widehat{m}_n}{m_n^0} - \widehat{E}_g^e \right) y' \right) + O(\kappa^2) = 0. \tag{B.8}$$

Likewise, we combine $(3.22)_3$, (B.3), and $(B.4)_2$, and introduce the variable

$$z := \overline{v} \exp[V] - 1 \tag{B.9}$$

to write the following equation for z on $(x_0, 1)$:

$$z'' - \frac{1}{(L_p^0)^2} z + \kappa \left(\frac{\widehat{m}_p}{m_p^0} (x - x_0) z'' + \left(\frac{\widehat{m}_p}{m_p^0} - \widehat{E}_g^e \right) z' \right) + O(\kappa^2) = 0, \tag{B.10}$$

where $L_p^0 := \sqrt{\tau_p m_p^0}$ is the diffusion length of holes.

We solve (B.8) by posing the following Poincaré asymptotic expansion:

$$y(x) = y_0(x) + \kappa y_1(x) + O(\kappa^2), \tag{B.11}$$

which we substitute in (B.8). At orders 0 and 1 in κ, we obtain the following equations on $(0, x_0)$:

$$\begin{cases} O(\kappa^0): & y_0'' - \dfrac{1}{(L_n^0)^2} y_0 = 0, \\ O(\kappa^1): & y_1'' - \dfrac{1}{(L_n^0)^2} y_1 = -\left(\dfrac{\widehat{m}_n}{m_n^0} (x - x_0) y_0'' + \left(\dfrac{\widehat{m}_n}{m_n^0} - \widehat{E}_g^e \right) y_0' \right), \end{cases} \tag{B.12}$$

along with the boundary conditions

$$\begin{cases} y_0(0) = 0, & y_0(x_0) = \exp[V] - 1, \\ y_1(0) = 0, & y_1(x_0) = 0. \end{cases} \tag{B.13}$$

The resolution of (B.12) yields, for $x \in (0, x_0)$,

$$\begin{cases} y_0(x) = \left(\exp[V] - 1 \right) \dfrac{\sinh\left(\dfrac{x}{L_n^0} \right)}{\sinh\left(\dfrac{x_0}{L_n^0} \right)}, \\ y_1(x) = -\dfrac{\exp[V] - 1}{8 L_n^0 \sinh\left(\dfrac{x_0}{L_n^0} \right)} \left[\cosh\left(\dfrac{x}{L_n^0} \right) \left(\dfrac{\widehat{m}_n}{m_n^0} 2x(x - 2x_0) \right) \right. \\ \qquad \left. + \sinh\left(\dfrac{x}{L_n^0} \right) \left(-4 \widehat{E}_g^e L_n^0 (x - x_0) + \dfrac{\widehat{m}_n}{m_n^0} \left(2 L_n^0 (x - x_0) + 2 \coth\left(\dfrac{x_0}{L_n^0} \right) x_0^2 \right) \right) \right]. \end{cases} \tag{B.14}$$

Similarly, (B.10) is solved with the asymptotic expansion:

$$z(x) = z_0(x) + \kappa z_1(x) + O(\kappa^2). \tag{B.15}$$

At orders 0 and 1 in κ we obtain the following equations on $(x_0, 1)$:

$$\begin{cases} O(\kappa^0): & z_0'' - \dfrac{1}{(L_p^0)^2} z_0 = 0, \\ O(\kappa^1): & z_1'' - \dfrac{1}{(L_p^0)^2} z_1 = -\left(\dfrac{\widehat{m}_p}{m_p^0} (x - x_0) z_0'' + \left(\dfrac{\widehat{m}_p}{m_p^0} - \widehat{E}_g^e \right) z_0' \right), \end{cases} \tag{B.16}$$

along with the boundary conditions

$$\begin{cases} z_0(x_0) = \exp[V] - 1, & z_0(1) = 0, \\ z_1(x_0) = 0, & z_1(1) = 0. \end{cases} \tag{B.17}$$

The resolution of (B.16) yields, for $x \in (x_0, 1)$,

$$\begin{cases} z_0(x) = \left(\exp[V]-1\right)\dfrac{\sinh\left(\dfrac{1-x}{L_p^0}\right)}{\sinh\left(\dfrac{1-x_0}{L_p^0}\right)}, \\ z_1(x) = \dfrac{\exp[V]-1}{8L_p^0\sinh\left(\dfrac{1-x_0}{L_p^0}\right)}\Bigg[-\cosh\left(\frac{1-x}{L_p^0}\right)\left(\frac{\widehat{m}_p}{m_p^0}2(1-x)(x-2x_0+1)\right) \\ \qquad + \sinh\left(\frac{1-x}{L_p^0}\right)\left(4\widehat{E}_g^e L_p^0(x-x_0)+\frac{\widehat{m}_p}{m_p^0}\left(-2L_p^0(x-x_0)+2\coth\left(\frac{1-x_0}{L_p^0}\right)(1-x_0)^2\right)\right)\Bigg]. \end{cases} \tag{B.18}$$

We now know the functions y and z on $(0, x_0)$ and $(x_0, 1)$, respectively. Hence, combining (B.5), (B.7), (B.9), (B.11), (B.14), (B.15), and (B.18), we obtain an explicit expression for $\bar{u}$ and $\bar{v}$ on (0, 1) (which we do not report here for the sake of brevity). We can combine (B.4) with these expressions of $\bar{u}$ and $\bar{v}$ to compute the currents of electrons and holes in the minority carrier regions. The currents, when evaluated at x_0^- and x_0^+ for $\jmath_n$ and $\jmath_p$, are given in (3.30).

References

Adams, A.R., 2011. Strained-layer quantum-well lasers. IEEE J. Sel. Top. Quantum Electron. 17 (5), 1364–1373. doi:10.1109/jstqe.2011.2108995.

Bardeen, J., Shockley, W., 1950. Deformation potentials and mobilities in non-polar crystals. Phys. Rev. 80 (1), 72–80. doi:10.1103/physrev.80.72.

Barlian, A., Park, W.-T., Mallon, J., Rastegar, A., Pruitt, B., 2009. Review: semiconductor piezoresistance for microsystems. Proc. IEEE 97 (3), 513–552. doi:10.1109/jproc.2009.2013612.

Bir, G.L., Pikus, G.E., Shelnitz, P., Louvish, D., 1974. Symmetry and Strain-Induced Effects in Semiconductors, 624. Wiley, New York.

Chadwick, P., 1976. Continuum Mechanics. Wiley, New York.

Chu, M., Sun, Y., Aghoram, U., Thompson, S.E., 2009. Strain: a solution for higher carrier mobility in nanoscale MOSFETs. Ann. Rev. Mater. Res. 39 (1), 203–229. doi:10.1146/annurev-matsci-082908-145312.

Coleman, B.D., Noll, W., 1963. The thermodynamics of elastic materials with heat conduction and viscosity. Arch. Ration. Mech. Anal. 13 (1), 167–178. doi:10.1007/BF01262690.

Coleman, J., 2000. Strained-layer inGaAs quantum-well heterostructure lasers. IEEE J. Sel. Top. Quantum Electron. 6 (6), 1008–1013. doi:10.1109/2944.902149.

Creemer, J., French, P., 2000. The piezojunction effect in bipolar transistors at moderate stress levels: a theoretical and experimental study. Sens. Actuat. A Phys. 82 (1–3), 181–185. URL: http://www.sciencedirect.com/science/article/pii/S0924424799003623.

Creemer, J.F., 2002. The Effect of Mechanical Stress on Bipolar Transistor Characteristics. Ph.D. thesis. Delft University of Technology.

Creemer, J.F., Fruett, F., Meijer, G.C.M., French, P.J., 2001. The piezojunction effect in silicon sensors and circuits and its relation to piezoresistance. IEEE Sens. J. 1 (2), 98. doi:10.1109/JSEN.2001.936927.

Ding, X., Ko, W.H., Mansour, J.M., 1990. Residual stress and mechanical properties of boron-doped p+-silicon films. Sens. Actuat. A Phys. 23 (1), 866–871. doi:10.1016/0924-4247(90)87048-N. URL http://www.sciencedirect.com/science/article/pii/092442479087048N.

Ericson, F., Schweitz, J.-A., 1990. Micromechanical fracture strength of silicon. J. Appl. Phys. 68 (11), 5840–5844. doi:10.1063/1.346957.

Fischetti, M.V., Laux, S.E., 1996. Band structure, deformation potentials, and carrier mobility in strained Si, Ge, and SiGe alloys. J. Appl. Phys. 80 (4), 2234. doi:10.1063/1.363052.

Fonash, S., 2012. Solar Cell Device Physics. Elsevier.

Freund, L., Johnson, H., 2001. Influence of strain on functional characteristics of nanoelectronic devices. J. Mech. Phys. Solids 49 (9), 1925–1935. doi:10.1016/S0022-5096(01)00039-4. The {JW} Hutchinson and {JR} Rice 60th Anniversary Issue.

Fried, E., Gurtin, M.E., 1999. Coherent solid-state phase transitions with atomic diffusion: a thermomechanical treatment. J. Stat. Phys. 95 (5), 1361–1427. doi:10.1023/A:1004535408168.

Fried, E., Gurtin, M.E., 2004. A unified treatment of evolving interfaces accounting for small deformations and atomic transport with emphasis on grain-boundaries and epitaxy. Adv. Appl. Mech. 40, 1–177. doi:10.1016/S0065-2156(04)40001-5. URL: http://www.sciencedirect.com/science/article/pii/S0065215604400015.

Friedel, P., Hybertsen, M.S., Schlüter, M., 1989. Local empirical pseudopotential approach to the optical properties of Si/Ge superlattices. Phys. Rev. B 39, 7974–7977. doi:10.1103/PhysRevB.39.7974.

Goddard, J.D., 2011. On the thermoelectricity of W. Thomson: towards a theory of thermoelastic conductors. J. Elast. 104 (1), 267–280. doi:10.1007/s10659-011-9309-6.

Gurtin, M.E., Vargas, A.S., 1971. On the classical theory of reacting fluid mixtures. Arch. Ration. Mech. Anal. 43 (3), 179–197. doi:10.1007/BF00251451.

Herring, C., Vogt, E., 1956. Transport and deformation-potential theory for many-valley semiconductors with anisotropic scattering. Phys. Rev. 101 (3), 944–961. doi:10.1103/physrev.101.944.

Johnson, H., Freund, L., 2001. The influence of strain on confined electronic states in semiconductor quantum structures. Int. J. Solids Struct. 38 (6–7), 1045–1062. doi:10.1016/S0020-7683(00)00072-X. URL: http://www.sciencedirect.com/science/article/pii/S002076830000072X.

Johnson, H.T., Freund, L.B., Akyz, C.D., Zaslavsky, A., 1998. Finite element analysis of strain effects on electronic and transport properties in quantum dots and wires. J. Appl. Phys. 84 (7), 3714–3725. doi:10.1063/1.368549. URL: http://scitation.aip.org/content/aip/journal/jap/84/7/10.1063/1.368549.

Kanda, Y., 1967. Effect of stress on germanium and silicon $p-n$junctions. Jpn. J. Appl. Phys. 6 (4), 475.

Kanda, Y., 1991. Piezoresistance effect of silicon. Sens. Actuat. A Phys. 28 (2), 83–91. doi:10.1016/0924-4247(91)85017-i.

Kittel, C., 2004. Introduction to Solid State Physics, eighth Wiley, New York.

Kittel, C., Kroemer, H., 1980. Thermal Physics. Macmillan.

Kleimann, P., Semmache, B., Le Berre, M., Barbier, D., 1998. Stress-dependent hole effective masses and piezoresistive properties of p-type monocrystalline and polycrystalline silicon. Phys. Rev. B 57, 8966–8971. doi:10.1103/PhysRevB.57.8966.

Kovetz, A., 2000. Electromagnetic Theory. Oxford University Press, Oxford.

Kroemer, H., 1957. Quasi-electric and quasi-magnetic fields in nonuniform semiconductors. RCA Rev. 18 (3), 332–342.

Lange, D., i Cabarrocas, P.R., Triantafyllidis, N., Daineka, D., 2016. Piezoresistivity of thin film semiconductors with application to thin film silicon solar cells. Solar Energy Mater. Solar Cells 145, 93–103. doi:10.1016/j.solmat.2015.09.014. Selected papers of the {EMRS} 2015 Spring meeting Symposium C on Advanced Inorganic Materials and Structures for Photovoltaics, URL: http://www.sciencedirect.com/science/article/pii/S092702481500447X.

de Lorenzi, H.G., Tiersten, H.F., 1975. On the interaction of the electromagnetic field with heat conducting deformable semiconductors. J. Math. Phys. 16 (4), 938–957. doi:10.1063/1.522600. URL http://scitation.aip.org/content/aip/journal/jmp/16/4/10.1063/1.522600.

Manku, T., Nathan, A., 1993. Electrical properties of silicon under nonuniform stress. J. Appl. Phys. 74 (3), 1832–1837. doi:10.1063/1.354790. URL http://scitation.aip.org/content/aip/journal/jap/74/3/10.1063/1.354790.

Markowich, P., Ringhofer, C., Schmeiser, C., 1990. Semiconductor Equations. Springer-Verlag, Wien, New York.
Markowich, P.A., 1986. The Stationary Semiconductor Device Equations. Springer-Verlag Wien, New York.
Markowich, P.A., Ringhofer, C.A., 1984. A singularly perturbed boundary value problem modelling a semiconductor device. SIAM J. Appl. Math. 44 (2), 231–256. doi:10.1137/0144018.
Marshak, A.H., Vliet, C.M.V., 1984. Electrical current and carrier density in degenerate materials with nonuniform band structure. Proc. IEEE 72 (2), 148–164. doi:10.1109/PROC.1984.12836.
Marshak, A.H., van Vliet, K.M., 1978. Electrical current in solids with position-dependent band structure. Solid-State Electron. 21 (2), 417–427. doi:10.1016/0038-1101(78)90272-1. URL: http://www.sciencedirect.com/science/article/pii/0038110178902721.
Müller, I., 1968. A thermodynamic theory of mixtures of fluids. Arch. Ration. Mech. Anal. 28 (1), 1–39. doi:10.1007/BF00281561.
Najafi, K., Suzuki, K., 1989. Measurement of fracture stress, Young's modulus, and intrinsic stress of heavily boron-doped silicon microstructures. Thin Solid Films 181 (1), 251–258. doi:10.1016/0040-6090(89)90492-6. URL http://www.sciencedirect.com/science/article/pii/0040609089904926.
Nelson, J., 2003. The Physics of Solar Cells, 1. Imperial College Press, UK.
Pierret, R.F., 1987. Advanced Semiconductor Fundamentals, 6. Addison-Wesley, Reading, MA.
Please, C.P., 1982. An analysis of semiconductor $p-n$ junctions. IMA J. Appl. Math. 28 (3), 301–318. doi:10.1093/imamat/28.3.301. URL: http://imamat.oxfordjournals.org/content/28/3/301.full.pdf+html.
Selberherr, S., 1984. Analysis and Simulation of Semiconductor Devices. Springer, Vienna doi:10.1007/978-3-7091-8752-4.
Shockley, W., 1949. The theory of $p-n$ junctions in semiconductors and $p-n$junction transistors. Bell Syst. Tech. J. 28 (3), 435–489. doi:10.1002/j.1538-7305.1949.tb03645.x.
Smith, C.S., 1954. Piezoresistance effect in germanium and silicon. Phys. Rev. 94 (1), 42–49. doi:10.1103/physrev.94.42.
Steigmann, D.J., 2009. On the formulation of balance laws for electromagnetic continua. Math. Mech. Solids 14 (4), 390–402. doi:10.1177/1081286507080808.
Sze, S.M., Ng, K.K., 2006. Physics of Semiconductor Devices. John Wiley & Sons.
Tadmor, E.B., Miller, R.E., Elliott, R.S., 2012. Continuum Mechanics and Thermodynamics: From Fundamental Concepts to Governing Equations. Cambridge University Press.
Thompson, S., Armstrong, M., Auth, C., Alavi, M., Buehler, M., Chau, R., Cea, S., Ghani, T., Glass, G., Hoffman, T., Jan, C.-H., Kenyon, C., Klaus, J., Kuhn, K., Ma, Z., Mcintyre, B., Mistry, K., Murthy, A., Obradovic, B., Nagisetty, R., Nguyen, P., Sivakumar, S., Shaheed, R., Shifren, L., Tufts, B., Tyagi, S., Bohr, M., El-Mansy, Y., 2004. A 90-nm logic technology featuring strained-silicon. IEEE Trans. Electron Devices 51 (11), 1790–1797. doi:10.1109/ted.2004.836648.
Thompson, S., Sun, G., Choi, Y.S., Nishida, T., 2006. Uniaxial-process-induced strained-Si: extending the CMOS roadmap. IEEE Trans. Electron Devices 53 (5), 1010–1020. doi:10.1109/ted.2006.872088.
Van de Walle, C.G., 1989. Band lineups and deformation potentials in the model-solid theory. Phys. Rev. B 39, 1871–1883. doi:10.1103/PhysRevB.39.1871.
Wortman, J.J., Evans, R.A., 1965. Young's modulus, Shear modulus, and Poisson's ratio in silicon and germanium. J. Appl. Phys. 36 (1), 153. doi:10.1063/1.1713863.
Wortman, J.J., Hauser, J.R., 1966. Effect of mechanical stress on $p-n$ junction device characteristics: II. Generation recombination current. J. Appl. Phys. 37 (9), 3527–3530. doi:10.1063/1.1708894. URL: http://scitation.aip.org/content/aip/journal/jap/37/9/10.1063/1.1708894.
Wortman, J.J., Hauser, J.R., Burger, R.M., 1964. Effect of mechanical stress on $p-n$ junction device characteristics. J. Appl. Phys. 35 (7), 2122–2131. doi:10.1063/1.1702802. URL: http://scitation.aip.org/content/aip/journal/jap/35/7/10.1063/1.1702802.
Xiao, Y., Bhattacharya, K., 2008. A continuum theory of deformable, semiconducting ferroelectrics. Arch. Ration. Mech. Anal. 189 (1), 59–95. doi:10.1007/s00205-007-0096-y.
Xu, S., Yan, Z., Jang, K.-I., Huang, W., Fu, H., Kim, J., Wei, Z., Flavin, M., McCracken, J., Wang, R., Badea, A., Liu, Y., Xiao, D., Zhou, G., Lee, J., Chung, H.U., Cheng, H., Ren, W., Banks, A., Li, X., Paik, U., Nuzzo, R.G., Huang, Y., Zhang, Y., Rogers, J.A., 2015. Assembly of micro/nanomaterials into complex, three-dimensional architectures by compressive buckling. Science 347 (6218), 154–159. doi:10.1126/science.1260960. http://science.sciencemag.org/content/347/6218/154.full.pdf.